NON-INTRUSIVE MEASUREMENT OF PARTICLE CHARGE: ELECTROSTATIC DRY COAL CLEANING

HENG BAN, JOHN L. SCHAEFER AND JOHN M. STENCEL
CENTER FOR APPLIED ENERGY RESEARCH
3572 IRON WORKS PIKE
LEXINGTON, KY 50511

ABSTRACT

Fundamental information on triboelectrification and electrostatic separation of coal and representative mineral matter was obtained. This bench-scale work quantified the charge and charge distribution imparted on coals, silica, alumina, pyrite and other particulate mixtures as a function of their size and velocity within Cu loops and mixer tribochargers. The charge was also measured for these samples at temperatures between 25-140°C and relative humidity between 0-70%.

INTRODUCTION

Dry coal cleaning technologies have not been investigated to the extent of wet coal cleaning technologies. A potentially attractive dry coal cleaning process is electrostatic separation, which depends on establishing a differential charge between the finely ground coal and mineral matter particles. Such differential charge is not imparted by ion bombardment (corona charging) or induction methods, but can be imparted by contact or frictional (triboelectrification) techniques. For triboelectrification, the magnitude and sign of the charge on a particle depends on the difference between the work functions or Fermi energy levels of the particle and that material or particle which was contacted[1]. The material with lower work function tends to lose electrons when in contact with a higher work function material.

There has been some development work to design process flow equipment for electrostatic cleaning of coal [2-4]. Link, et al.[5], and recently Finseth, et al.[6,7], have examined bench scale triboelectric separation for coal cleaning and have offered key insight into its possibilities.

There is yet a need to understand and to quantify particle charge characteristics and the physical and/or chemical factors of particles and processing that would impact coal-mineral matter separation. The current research investigated characteristics of coal particle charging and the effects of processing conditions.

EXPERIMENTAL

Experiments were conducted using coals and constituent/representative minerals, including pyrite, alumina, glassy carbon, and well-characterized and spherical silica. The characteristics of these samples are presented in Table 1.

The coals and minerals were crushed under wet conditions, and wet sieved to provide a -200+325 mesh (75-48 micrometers) and -140/+200 mesh (106-75 micrometers) fractions. The samples were dried in a vacuum oven at 110°C for 10 hours and then stored in Ar purged containers until use.

The experimental apparatus used in the triboelectrostatic testing is depicted in Figure 1. The feed system consisted of an enclosed vibratory feeder which was purged with the separation chamber gas, an injector, a tribocharging loop constructed of 6 mm diameter Cu tubing, and a ceramic transport tube which delivered the charged particles to the separation chamber. The gas velocity within the tribocharging loop was varied between 5-40 m/s.

The separation chamber consisted of parallel Cu plates separated by 10 cm, between which a high voltage potential was applied. At the end of the chamber was a filter and an induced draft line. This equipment was connected to an X-Y positioner which was in turn mounted on a optical table along with the laser, phase Doppler particle analyzer (PDPA).

Samples passing through the parallel plates of the separator were examined real-time and on-line by the PDPA. The X-Y positioner was used to control the position of the separation chamber and, hence, to move the laser, PDPA probe volume horizontally across the chamber at a speed of 0.1 mm/s.

After an experimental run, particles that had been charged and deposited on the positive (anode) or negative (cathode) plates were scraped into a basket placed at the bottom of the respective plate. Uncharged particles flowed downward through the center of the plates and were captured during the runs on a 325 mesh (48 μm) screen placed at the bottom and exit of the separation chamber.

Besides PDPA instrumentation, the charge imparted on samples within the Cu tribocharger was obtained by measuring the induced charge for particles captured in a Faraday cage, the current flow to a tribocharger during particulate flow, and the current produced as a consequence of capturing charged particles in a ionic solution.

RESULTS AND DISCUSSION

Figure 2 illustrates the change in the absolute value and distribution of charge on silica particles as a consequence of changing the tribocharging velocity. As the velocity was increased, the average charge imparted on the particles and the width of the charge distribution increased. This result is general for all samples which have been investigated. In addition, it is to be noted that the charge distributions contain both negatively and positively charged particles. For coal particles, and when using Cu as the tribocharging surface, a positive charge was expected, whereas for minerals a negative charge was expected. Also, the data in Figure 2 show that there are more particles having reversed charge under conditions

leading to greater average charge values. Such charge reversal is probably related to electrical induction which is a consequence of particle-to-particle or particle-to-separator plate contacts.

The data in Figures 3 and 4 show that, for Elswick seam coal, the average charge imparted on the coal particles is nearly linearly dependent on the charging velocity. In addition, particles having a -200/+325 mesh size range attained a greater charge/mass ratio than did particles having a -140/+200 mesh size range. Increased particle charge with increased charging velocity was also observed for pyrite (see Figures 5 and 6). In agreement with the data in Figure 3 and 4, the pyrite data shows greater charge/mass ratios for the smaller (-200/+325 mesh) particles than for the larger (-140/+200 mesh) particles. The absolute value of this size-dependent difference was dependent, however, on the feeding rate to the tribocharger.

The current flowing to the tribocharger as the temperatures of the charger and carrier gas were increased is shown in Figures 7 and 8 for Elswick seam coal. For these samples, the current (and hence the charge imparted on the coal) was independent of the temperature of charging between 25-140°C. However, data in for silica particles show that an increase in the temperature of charging cause a decrease in the current flow. In the case of the coal, it is possible that partial drying of the particles occurred at the higher temperatures, thereby enabling either constant or slightly increased charge accumulation.

It is generally accepted that charging of nonconducting materials by triboelectrification involves the surface of the material and its unique surface sites[8]. Surface sites or states, eg. electronic levels, should not be altered significantly over the relatively small temperature changes which we have investigated. However, if moisture or the extent of hydration was involved in the charging or discharging mechanism, or in the formation and form of the surface site, then it is possible that small temperature changes would affect significantly the charge which was measured during triboelectrification. However, an increase in temperature decreased the charge accumulated on the silica particles but did not affect charge accumulated on coal particles. The examination of the charging and discharging characteristics of coal and mineral constituents is continuing.

CONCLUSIONS

It is possible to examine the behavior and charging characteristics of coal and constitutent minerals to develop fundamental information relating to dry coal separation by electrostatic conditions. Tribocharing using a Cu surface imparts a positive charge on the carbon and a negative charge on the mineral in coals. Reversed-sign charging is related to induction and is more pronounced the greater the charge accumulation. The effects of coal processing conditions, typical to that in feed streams to pulverized coal combustors, on the

electrostatic cleaning of coals are to be examined further in future planned experimentation.

ACKNOWLEDGEMENTS

Partial funding from the U.S.D.o.E., Grant DE-FG22-91PC91290, and the Commonwealth of Kentucky through its Center for Applied Energy Research, are gratefully acknowledged. The assistance of J. Hower in obtaining the coal samples is also gratefully acknowledged.

REFERENCES

1. Labadz, A. F. and Lowell, J. Journal of Electrostatics, 1991, **26**, 251.
2. Shih, Y. T., Gidaspow, D. and Wasan, D. AIChE J. 1987, **33**, 8, 1322.
3. Gupta, R. Ph. D. Dissertation, Ill. Inst. of Tech., 1990.
4. Inculet, I. I., Quigley, R. M. and Faurschou, D. K. CIM Bulletin, Coal Research Oct. 1980, **73**, 51.
5. Link, A. T., Killmeyer, R., Elstrodt, R. and Haden, N. USDoE PETC Report, 1990, DOE/PETC/TR-90/1.
6. Finseth, D., Newby, T. and Elstrodt, R. Preprint, 5th, Int. Conf. Proc. & Util. of High Sulfer Coals Oct. 1993, Lexington, Kentucky, USA.
7. Finseth, D. et al. personal communication.
8. E.G. Kelly and D.J. Spottiswood, Min. Eng., 2, 193(1989).

Table 1. Coal characteristics for Leatherwood seam, Harlan County, KY and Elswich seam, Pike County, KY (-200+325 mesh).

	Moisture	Ash	% Volatiles	Fixed Carbon
Leatherwood	1.7	10.7	33.9	53.7
Elswick	0.9	11.8	52.9	34.5

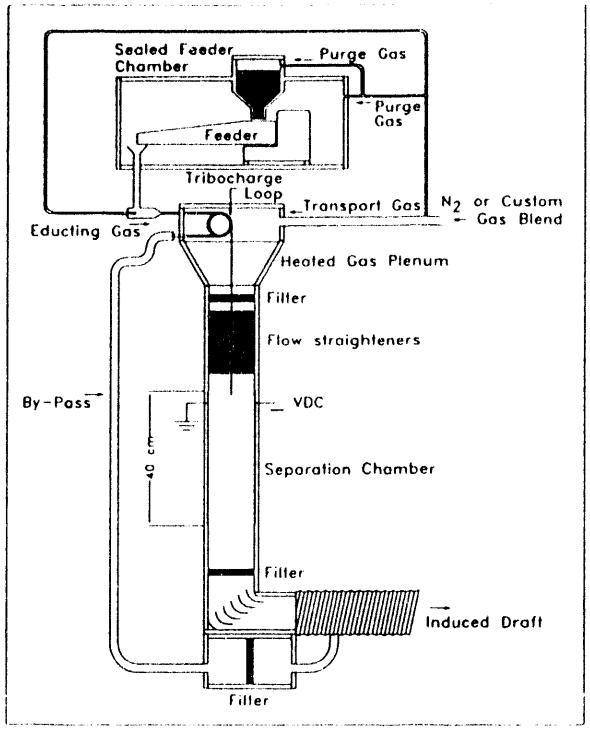

Figure 1. Experimental apparatus to tribocharge and electrostatically separate finely ground coal under laminar flow conditions.

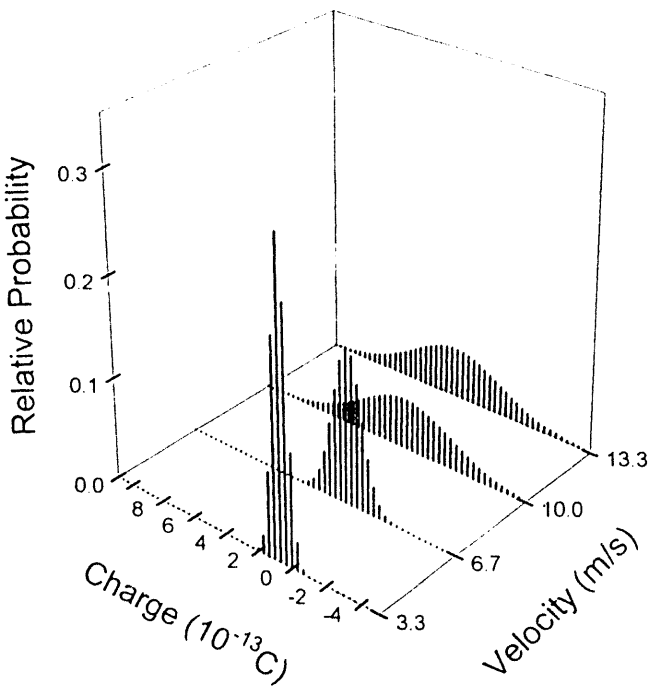

Figure 2. The value and distribution of charge established on silica particles during triboelectrification at room temperature.

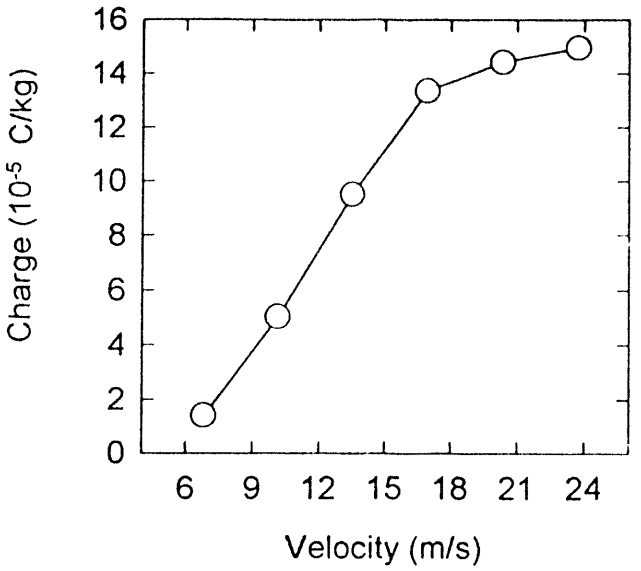

Figure 3: The effect of velocity on average coal (-200+325 mesh) charge in nitrogen environment. This is a high volatile A, high rank bituminous coal from Elswick seam, Pike Co., KY.

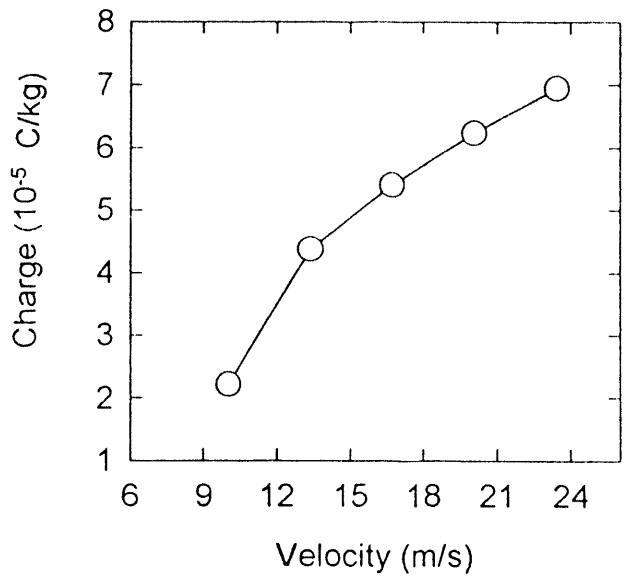

Figure 4: The effect of velocity on average coal (-140+200 mesh) charge in nitrogen environment. This is a high volatile A, high rank bituminous coal from Elswick seam, Pike Co., KY.

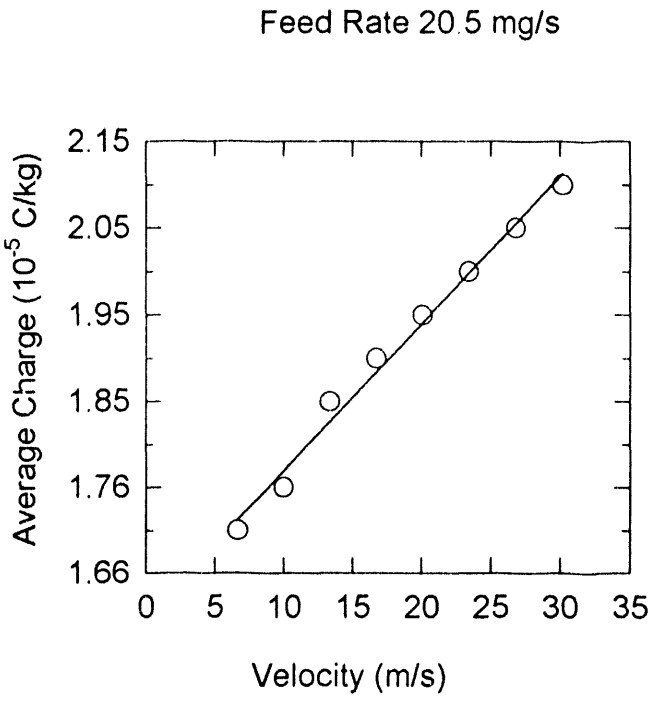

Figure 5. Average charge accumulated on pyrite relative to the charging velocity (-200+325 mesh).

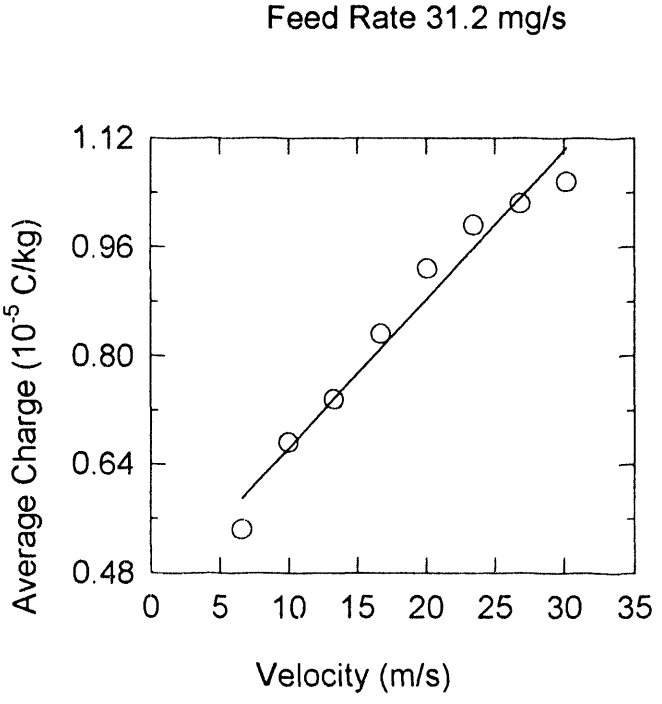

Figure 6. Average charge accumulated on pyrite relative to the charging velocity (-140+200 mesh).

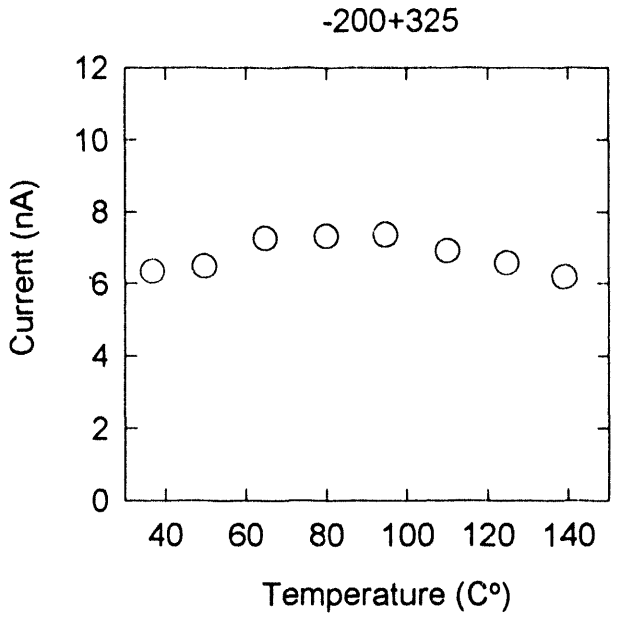

Figure 7. Current flow to tribocharger during charging of Elswick seam coal relative to increasing temperature (25 m/s).

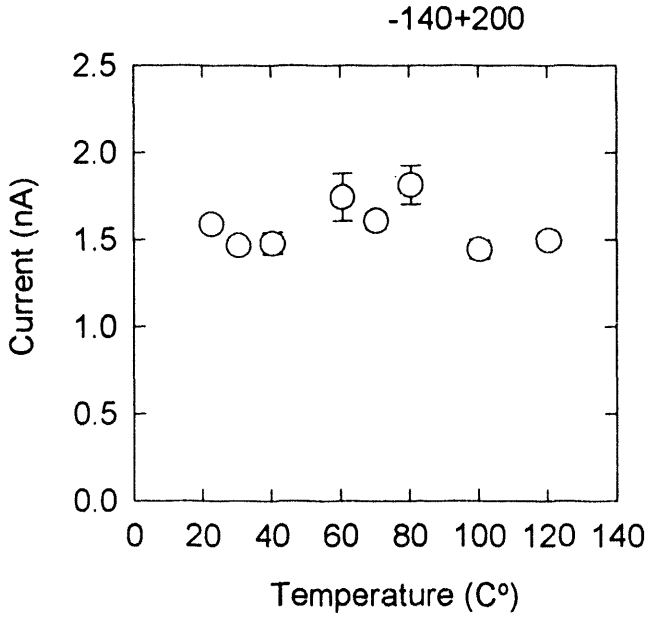

Figure 8. Current flow to tribocharger during charging of Elswick seam coal with increasing temperature (25 m/s).

DEVELOPMENT OF THE TRIBO-ELECTROSTATIC FINE COAL SEPARATOR

William D. Gerstler, Postgraduate Fellow
Oak Ridge Associated Universities

Dennis H. Finseth, Senior Physical Scientist
U.S. Department of Energy
Pittsburgh Energy Technology Center
P.O Box 10940
Pittsburgh, Pennsylvania 15236

INTRODUCTION:

Tribo-electrostatic coal cleaning is a physical method for removing impurities from fine dry coal. The process utilizes the difference in electrical charging characteristics between the clean burning organic material and the mineral matter [1],[2]. Because the mineral matter contains many harmful impurities found in run-of-mine coal, removing it from the organic material can significantly reduce emissions [3],[4]. The goal of this study is to develop a continuous process which cleans dry coal powder, thereby eliminating the need for the energy intensive dewatering step in classical wet separation [1],[2]. The study is simultaneously approaching the problem from the fundamental and practical perspectives.

Physical coal beneficiation requires liberation of organic material from mineral matter [3],[5]. Past work indicates that grinding the coal to minus 200 Mesh (below 75 μm) results in effective liberation for tribo-electrostatic separation. There are three basic elements required for an electrostatic dry powder separating system: a particle charger, a separator, and a means to collect the separated material [1]. Figure 1 shows the general schematic for a tribo-electrostatic separator.

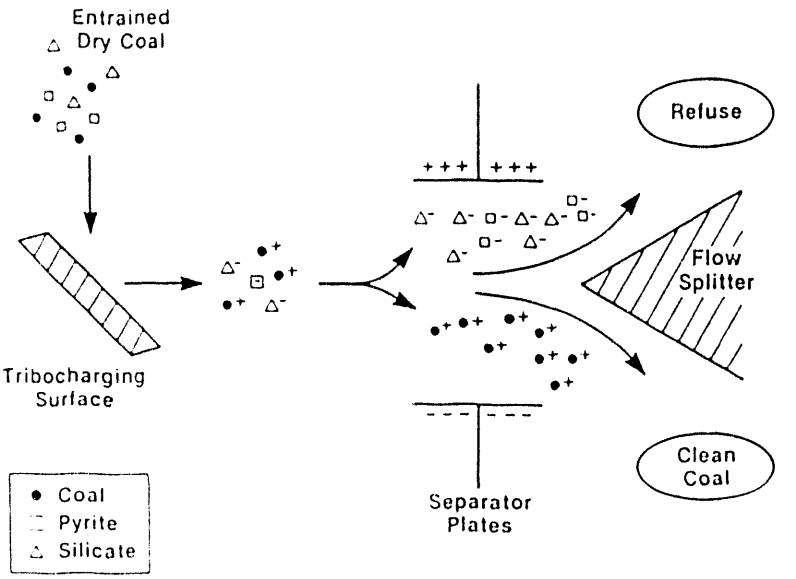

Figure 1. Schematic of Tribo-electrostatic Coal Separation

The coal, entrained in a stream of nitrogen carrier gas, collides with the surface of the charger under turbulent conditions. The organic material and the mineral matter acquire opposite charges (organic +, mineral -) and can be separated by a strong electric field.

The current study of tribo-electrostatic separations at PETC employs a continuous parallel plate unit, shown in Figure 2, which models the components of a large scale separator. To evaluate the process performance in more detail, an analytic batch unit with geometry identical to the continuous unit is used. In the analytic unit, coal fractions are not dislodged from the plates to the collection cyclones but collect on the electrode plates. The ash and sulfur compositions are then determined as a function of distance from the injector. Figure 3 shows typical deposition profiles and corresponding ash and pyritic sulfur compositions.

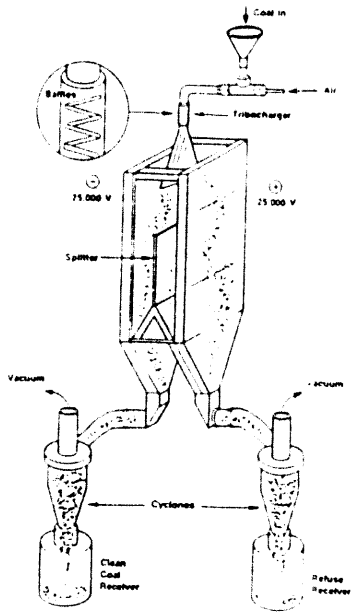

Figure 2. Schematic of the Continuous Tribo-Electrostatic Separator

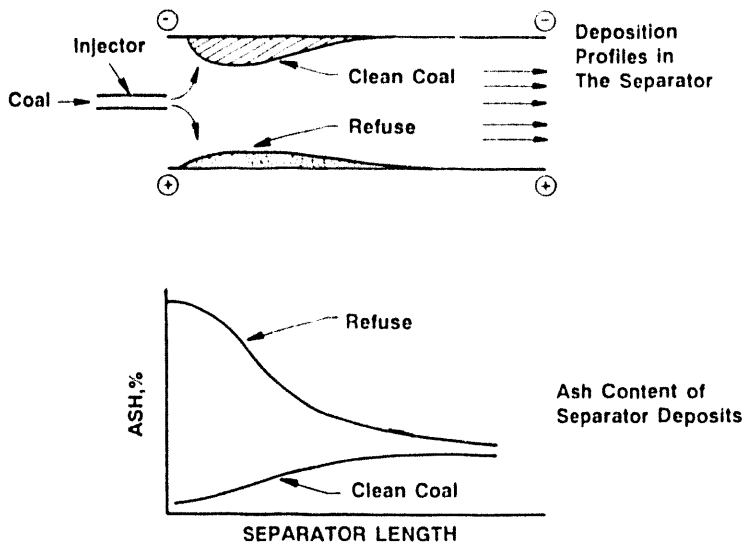

Figure 3. Representative Data for Analytic Separator

BACKGROUND:

For many years, electrostatic methods have been used to beneficiate dry material [5]. The majority of the commercial applications have been mineral separations. Other current uses include waste recycling and removing solid contaminants from bulk foods [6]. The methods commonly used to charge solid particles include induction, in which conductive particles acquire charge by touching grounded material within an electric field, and corona electrification, where all particles acquire a charge of the same polarity as they are exposed to ionic bombardment from the corona glow [5]. The use of these methods to clean coal has had very limited success [1],[2]. Recently, efforts have focused on charging by tribo-electrification, which involves surface contact, or rubbing, between two materials. The basic physics of tribo-charging is not well-understood for most materials, excepting pure metals [7]. Most fundamental research on insulators and semiconductors has been obtained on pure substances under highly controlled environments, and even then the results sometimes conflict [7],[8]. While basic mechanisms behind differential charging remain ambiguous, tribo-electrostatic separation has shown to be a viable means to separate mineral matter from coal [1],[2],[4],[5].

EXPERIMENTAL SETUP:

The focus of this paper is to determine the dependence of the separation performance on flow conditions and solids loading. Because of the need for detailed analysis of particle behavior, most work was performed using the analytic separator, which permits analysis of clean and refuse fraction subsets. Figure 4 shows a schematic of the analytic separator.

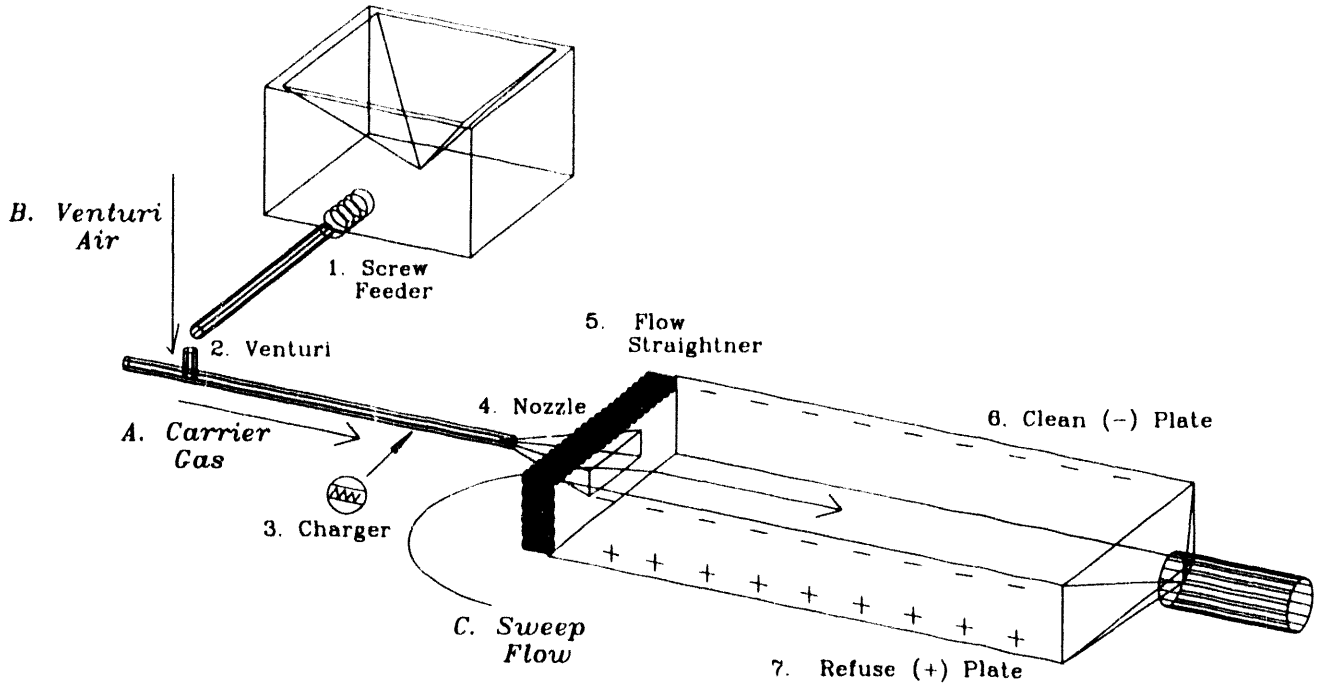

Figure 4. Schematic Design of the Analytic Separator

The following description of the process refers to Figure 4: The fine coal feed is placed in a volumetric screw feeder(1) where the solid loading rate is carefully controlled. The coal leaves the feeder and is entrained in a stream of nitrogen carrier gas using a venturi(2). The gas and particles move through a copper tube into a charger(3) consisting of a snugly placed copper in-line mixer. The turbulent conditions, generated by the mixer, causes selective charging of the material by contact with the copper. This is a simple and efficient means of charging particles, which requires no moving or mechanical parts [1].

The particles move into a triangular copper injector nozzle(4) that has an opening of about 6 inches by 1/8 inch. The charged particles leave the injector centered between the opening of two parallel copper plates 12 inches wide, placed 4 inches apart. These plates are charged with opposite polarities of 25 kV. A vacuum is applied to the end of the separator to draw sweep air through a 4-inch flow-straightening section(5) and into the separator section. The negatively charged inorganic material is attracted to the positive plate(6) while positively charged coal is directed to the negative plate(7).

RESULTS AND DISCUSSION:

1. Gas Flow in the Separator.

An important aspect of the investigation of electrostatic separation is the aerodynamics of the separator. An understanding of the particle-flow interactions, flow uniformity, and gas/particle ratios is essential to any effort to design a separator that can be scaled to work in a practical coal beneficiation environment. One focus of this study is to develop methods to measure these parameters which undoubtedly influence the quality of the separation.

The three fluid flows relevant to our separator configuration are shown in Figure 4. The nitrogen carrier gas(A) flow is kept constant (3.5 ft^3/min) by adjusting the driving pressure. Air drawn into the nitrogen stream with the solid particles by a venturi effect(B) varies from 0.12 ft^3 min to 2.3 ft^3/min depending on the rate of solids feed. Sweep air flow(C)is determined by subtracting the carrier and venturi flows from the total exit flow to the vacuum at the downstream end of the separator. This sweep flow is typically around 43 ft^3/min.

One of the most important parameters in the separator operations is the gas-to-solid mass ratio. If the separation process is to be effective on a large scale, it is vital to know the total air flow required, and if that amount is physically and economically practical. One possible process arrangement would couple the separator directly to a PC boiler which would require strict gas-to-solid mass ratios to insure proper air/fuel stoichiometry.

When we consider only the outlet of the injector, the gas-to-solid mass ratio using a coal feed rate of 10 lbs/hr is around 1.5:1. This mass ratio is not excessive for a practical separator and is within the range required by boiler stoichiometry (around 3:1, air/fuel). When the sweep flow is added, the ratio increases dramatically since the sweep flow constitutes 90 percent of total air flow. The large amount of sweep flow used in this work is due to laboratory safety concerns in dealing with fine coal dust. Previous tests have shown that satisfactory separations can be achieved at much lower sweep flow. We believe that the gas-to-solid mass ratio needed for efficient separation can be at least as low as 2:1. Current work is directed at demonstrating operability under these conditions.

Following measurement of the net volumetric flow parameters in the various parts of the separator, the spatial flow profiles of air exiting the injector and within the separation chamber were investigated. A velometer was used to measure the air flow velocities at various locations. Three dimensional velocity profiles, which assist in flow visualization, were made. To our knowledge, these are the first velocity profiles measured in a system of this type.

The velocity profile across the injector opening is not uniform, but is fairly symmetric with a peak velocity occurring on each side of center. The air leaving the injector combines with the slower sweep flow, resulting in the decrease of injector air velocity. After twenty inches, the two flow streams combine into one fairly symmetric flow moving approximately 2 m/s. The spatial gas flow pattern is highly sensitive to the positioning of the carrier gas inlet, therefore, care is taken to reproduce similar flow for each data run.

2. Variation of Separation with Solids Loading Rate

A commercially successful continuous coal separator must be capable of high throughput. Therefore, the variation of performance with respect to solid loading was investigated. Samples of pre-cleaned 200 x 0 mesh Pittsburgh #8 seam coal, with an ash content of 4.7 percent, total sulfur of 0.96 percent and pyritic sulfur of 0.22 percent were separated in the analytic unit using five feed rates ranging from 0.64 lbs/hr to 11.18 lbs/hr. The mass collection results are shown in Figure 5.

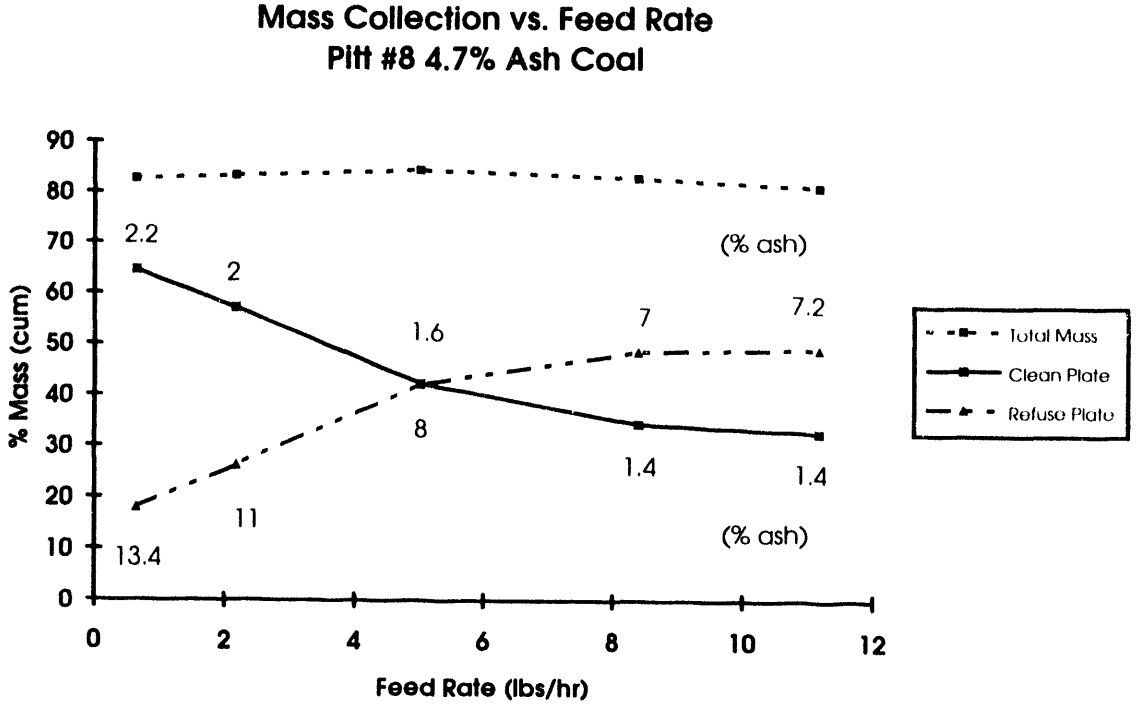

Figure 5. Mass Collection vs. Feed Rate

The total accumulated mass remains constant, indicating efficient charging even at high solids feed rate. Although total collection mass is constant, the plate to which the material migrates varies dramatically with feed rate. In an ideal system, all the organic material charges positive and collects on the clean plate, while mineral matter charges negative and collects on the refuse plate as indicated in Figure 1. Particle-to-particle collisions, particles containing both organic and mineral material, and space charges due to clouds of charged particles cause deviation from reality. Figure 6 schematically represents the recovery of ash and non-ash particles, on both the clean and refuse plate, for low and high feed rates.

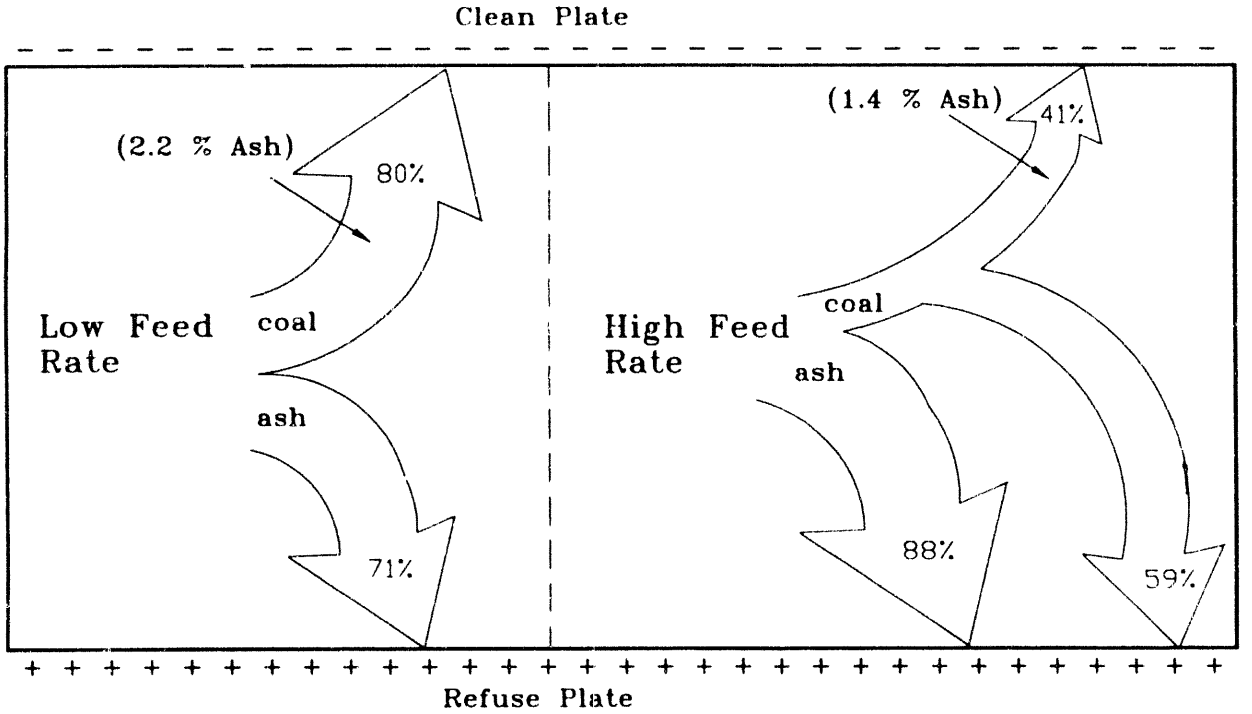

Figure 6. Schematic Representation of Coal and Ash Separation at Low and High Feed Rates

For this low ash coal, at low feed rates (0.64 lbs/hr), 80 percent of collected organic material migrates to the negative (clean) electrode resulting in a product with 2.2 percent ash. At high feed rates (11 lbs/hr), much of the same organic material moves to the positive (refuse) electrode resulting in only 41 percent of the organic material collecting on the clean plate. However, the product which collects on the clean plate has an ash content of only 1.4 percent. Therefore, increasing the feed rate diminishes the total recovery of coal on the clean plate, but the collected product can be up to 1/3 lower in ash content. Mineral matter collection on the refuse plate is enhanced by higher feed rates. At 0.64 lbs/hr, 71 percent of the collected ash goes to the refuse plate while at 11 lbs/hr, 88 percent collects on the refuse plate. These are totally new results from any previous work done at PETC. It should be noted that a duplicate set of tests were completed and the results were entirely reproducible.

Examining the mechanisms of particle tribo-charging and the frequency of different types of collisions under given feed conditions may explain this peculiar behavior. Figure 7 shows three charging possibilities for both clean coal particles and mineral matter, along with their relative probability of occurring at high and low feed rates.

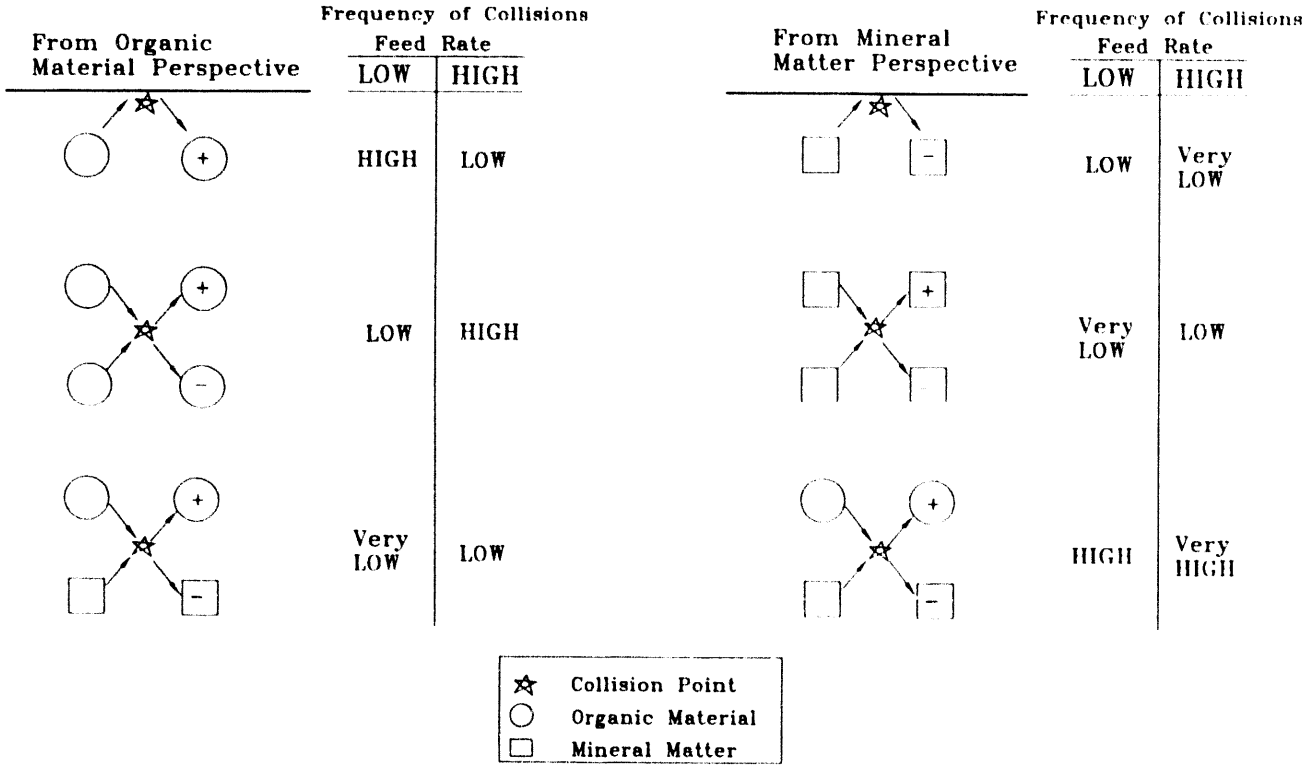

Figure 7. Schematic Representation of Particle Tribo-charging And The Relative Frequencies of Collisions

Our hypothesis is that at low feed rates particles are far apart and few particle-to-particle organic collisions occur. Under these conditions, the dominant charging of organic material is manifest by contact with copper, resulting in a positive charge and thereby sending them to the negative (clean) electrode. Those that migrate to the refuse side may do so because of unliberated mineral matter or one of the few collisions with like particles. At high feed rates, particle-to-particle collisions between organic material increase dramatically, causing many coal particles to charge negative and move to the refuse plate.

Because the feed coal is only 4.7 percent ash, particle-to-particle collisions involving mineral matter are primarily with coal particles. Thus for mineral matter, both charging mechanisms, particle-to-particle and particle-to-copper, result in the mineral acquiring a negative charge and depositing on the positive (refuse) plate. At high feed rates, the total number of collisions increases, hence the increased percentage of mineral depositing on the refuse plate. It should be mentioned that even at the highest feed rates, over 90 percent of the total pyritic sulfur is collected on the refuse plate. Optical microscopic analysis suggests that this represents virtually all the liberated pyrite.

The implications of this study for high throughput tribo-electric separation are that even at dense phase, the particles are charged and separation occurs. Even though the yield on the clean plate is low at high feed rates, the product is extremely clean (1.4 percent ash). Furthermore, if particle-to-particle charging is responsible for the misplaced clean coal at high feed rates, adding a recyclable solid charger to the feed to control the separation may be possible. In fact, previous work has suggested that adding silica to coal increases clean coal yield.

SUMMARY:
The flow rates and aerodynamics of the tribo-electrostatic separation process were investigated and the effects of feed rate variability were measured. Accomplishments and conclusions include:

1. Flow rates of all fluids and solids entering the separator are controlled and measured. Velocity profiles of injector air flow and flow within the separation chamber have been determined. This information permits calculation of accurate gas-to-solid mass ratios.

2. Low feed rates may cause the primary charging mechanism of organic material to be surface contact with copper, resulting in 80 percent of the collected coal to deposit on the clean plate. At higher feed rates, collisions between coal particles may begin to dominate organic material charging, causing many coal particles to charge negatively and move to the refuse plate. In this low ash coal, high feed rates enhance the already high percentage of mineral matter that deposits on the refuse plate. This is consistent with an increase in mineral-to-coal particle collisions, resulting in more effective charging of mineral particles.

3. It may be possible to manipulate the charging and separation of the clean coal by adding solid powders to instigate appropriate charging for the feed coal.

REFERENCES

[1] Dennis H. Finseth, Terri Newby and Robert Elstrodt, "Dry Electrostatic Separation of Fine Coal," Proc. of the (9th Korea-U.S. Joint Workshop On Coal Utilization Technology, October 1992.

[2] T. Link, R. Killmeyer, R. Elstrodt and N. Haden, "Initial Study of Dry Ultrafine Coal Beneficiation Utilizing Triboelectric Charging With Subsequent Electrostatic Separation," Project Report DOE/PETC/TR90/11, (DE91000943),October 1990.

[3] Kenneth E. Templemeyer et al., "Coal Refining: New Products from Illinois Coal Through Higher Technology Processing," Project Report, Southern Illinois University at Carbondale, March 1991.

[4] William D. Gerstler, "Beneficiation of Illinois Coal by Use of the Cylindrical Impact Electrostatic Separator," Masters Thesis, Southern Illinois University at Carbondale, 1992.

[5] Ion I. Inculet, Electrostatic Mineral Separation, John Wiley and Sons Inc., New York, 1984.

[6] A.D. Moore, Electrostatics and Its Applications, John Wiley and Sons Inc., New York, 1973.

[7] A.G. Bailey, "Charging of Solids and Powders," Journal of Electrostatics, 30 (1993) 167-180.

[8] A.R. Akande and J. Lowell, "Charge Transfer in Metal/Polymer Contacts," Journal of Applied Physics, 20 (1987) 565-578.

This publication is based on work performed in the Fossil Energy Postgraduate Research Training Program under Contract # DE-AC05-760R00033 between the U.S. Department of Energy and the Oak Ridge Institute for Science and Education.

SUPERCLEAN EMISSION SYSTEMS SESSION

FUNDAMENTAL MECHANISMS IN FLUE GAS CONDITIONING

Todd R. Snyder
Research Environmental Engineer

P. Vann Bush
Manager, Particulate Science and Engineering Group

Southern Research Institute
Birmingham, AL 35255-5305

Contract DE-AC22-91PC90365

The overall goal of this research project is to formulate a model describing effects of flue gas conditioning on particulate properties. This model will serve as a component of the performance models of particulate control devices where flue gas conditioning is used. By flue gas conditioning we mean any process by which solids, gases, or liquids are added to the combustor and/or the exhaust stream to the extent that flue gas and particulate properties may be altered. The model will be based on an understanding of how ash properties, such as cohesivity and resistivity, are changed by conditioning. Flue gas conditioning involves the modification of one or more of the parameters that determine the magnitude of forces acting on the fly ash particles, and can take place through many different methods. Modification of particulate properties can alter ash resistivity or ash cohesivity and result in improved control device performance. Changes to the flue gas, addition of particulate matter such as flue gas desulfurization (FGD) sorbents, or the addition of reactive gases or liquids can modify these properties. If we can better understand the mechanisms by which conditioning agents and FGD sorbents react with fly ash particles, application of appropriate conditioning agents may result in significantly improved fine particle collection at lower capital and operating costs.

THE ROLE OF ADSORBED LIQUID LAYERS IN INTERPARTICLE BONDING

Adsorbed water is an almost universal factor in the interaction of particles, even in cases of very low relative humidities[1]. Adsorption of water is specifically pertinent in the case of fly ash under virtually all flue gas conditions[2]. The form of the water depends on the relative humidity of the gas, the morphology of the particles, the geometry of the contact points, and the surface chemistry of the particles. Agents can be applied to particles to alter the affinity of their surfaces to water, and thereby affect the adhesion. Adsorbed water will form liquid bridges between particles when relative humidity exceeds some critical level for condensation to occur at contact points, reported to be between 65 and 80 %[3]. A meniscus forms around the point of contact between particles, and the surface tension of the liquid exerts a capillary force between particles.

We investigated fly ash conditioning and interparticle bonding forces in the laboratory. Because of the importance of liquid bridges in ash particle bonding, and because many of the various types of conditioning currently in use rely on liquid bridges to provide increased bonding strength, we concentrated on understanding and measuring liquid bridges on fly ashes and other powders. Since the most common material responsible for these adsorbed layers and liquid bridges is water, relative humidity was a key experimental parameter. Our data showed measurable effects of water vapor conditioning on bulk ash cohesivity, resistivity, and tensile strength. The degree to which ash resistivity was affected by water vapor conditioning depended on particle morphology and surface chemistry. Our measurements of tensile strength also demonstrated the effects of adsorbed water. As more water was adsorbed onto the ash samples, the tensile strength of samples also increased.

THE EFFECTS OF PARTICLE BONDING STRENGTH ON COLLECTION PROCESSES

In electrostatic precipitation electrical resistivity and cohesivity are two major properties of particulate matter that affect performance. Electrical resistivity of the collected material dictates the allowable current density that can be imposed on the material without causing electrical breakdown. Electrical breakdown in the collected particulate layer is the source of back corona (ionization within and from the collected layer) that can degrade charging and collection by ejecting neutralizing ions into the inter electrode region and by forcing operation at reduced voltages and corona currents. If electrical resistivity of a layer of particles is high enough ($\gg 10^{11}$ Ω-cm), the imposition it makes on operating voltages and currents can dramatically lower collection efficiency. If electrical resistivity is too low ($\ll 10^{8}$ Ω-cm), the charge on the particles and the applied electric field are insufficient to hold the particles on the collecting electrodes. The resulting phenomenon is called non-rapping, or electrostatic, reentrainment and can dramatically lower ESP collection efficiency.

Below about 400 °F the electrical resistivity of particulate matter can be decreased by lowering the temperature, or by adding some agent to the surface of the particles that enhances conduction of charge (water and SO_3 vapor are the most common additives that are used). Flue gas desulfurization systems that lower the gas temperature through cooling by evaporation of water, either as a constituent of a sorbent slurry or water spray, can produce conditions in ESPs at which the resistivity of the particulate matter is very low. SRI and others have documented cases of substantial non-rapping reentrainment in ESPs downstream of FGD systems[4]. A potential solution to this problem is to increase the cohesivity of the particulate matter.

Data show that increasing water content can increase tensile strength, which is one measure of cohesivity. Other conditioning agents, such as ammonia and SO_3 in combination, have been used to increase cohesivity of the particulate matter. Although the effects that lower electrical resistivity tend to increase cohesivity, usually the changes in resistivity are greater and the operating conditions in the ESP may still yield degraded performance. We believe that additional conditioning for the express purpose of increasing the cohesivity of the particulate matter can improve ESP performance by reducing or eliminating non-rapping reentrainment.

Ash characteristics affect filtering pressure drop, the removal of collected ash during cleaning cycles, and, in some cases, the overall collection efficiency of the fabric filter. Ash cohesivity plays a key role in each of these processes. Once stable operation (with constantly increasing filtering pressure drop) has been reached during a filtration cycle, the rate of increase of the pressure drop is entirely dependent on the characteristics of the particles being collected and the strength of the bonds between them. Darcy's Law, which describes the resistance to gas flow through a porous medium, indicates that particle morphology, specifically surface area, has a strong effect on pressure drop. (Resistance increases as the size of the particles decreases, or as the particles become rougher.) In general, flue gas conditioning has not been shown to significantly alter these aspects of particle morphology. Conditioning has been shown, however, to be quite effective in altering filter cake porosity, the other main characteristic of the cake that controls flow resistance. Porosity of a filter cake can be increased by the deposition of a liquid layer on the surfaces of the ash particles prior to their collection on the cake. The liquid layer increases the bonding strength between ash particles, and causes the particles to form an agglomerate with a higher porosity. Filtering pressure drop can be substantially reduced if filter cake porosity can be significantly increased.

Low ash cohesivity has been identified as the reason why ash particles gradually pass through the fabric at a few well-maintained baghouses. Although this problem is rare, it has been identified for some fly ashes. Pilot-scale work has shown that conditioning this ash with NH_3 and SO_3 causes the formation of liquid bridges (ammonium bisulfate) on the ash particles. The increased bonding strength between adjacent particles prevents significant penetration of ash through the fabric.

PILOT-SCALE TESTS TO VERIFY THE ROLES OF ADSORBED LIQUID

We are investigating two phenomena in our pilot-scale tests. The first is the ability of flue gas humidification to increase ash cohesivity through the creation of liquid bridges between particles collected in a fabric filter. Increasing cohesivity through the development of liquid bridges was demonstrated in our laboratory measurements of tensile strength and uncompacted bulk porosity, and in laboratory filtration studies performed for DOE/PETC under an earlier contract. With the range of coals fired in Southern Research Institute's Coal Combustion Facility (CCF), our filtration tests should verify how different fly ashes react to water conditioning in actual flue gas environments. We are drawing a slipstream of flue gas and entrained fly ash particles during several different CCF tests. Our laboratory studies indicated that the response of different types of fly ashes to water vapor conditioning varied greatly. The effects of actual flue gas, a variety of coals, and true size distributions of entrained fly ash particles should provide rigorous verification of the effects of developing liquid bridges. Any effects that adsorbed water has on ash cohesivity should be apparent in the fundamental gas-flow resistance (K_2) values measured during filtration cycles in a portable fabric filter.

We are also studying electrostatic reentrainment of previously collected ash particles in an ESP. We prepared a small ESP for use in our laboratory studies. These studies have shown the effects that relative humidity can have on the forces (resistivity, cohesivity, and tensile strength) that hold the collected ash on the grounded ESP plate. Severe reentrainment can occur when these three forces have been modified by changes in flue gas temperature and/or water content. Therefore we have been intentionally modifying these factors in order to induce this type of electrostatic reentrainment.

Facilities and Equipment

The design of Southern Research Institute's CCF provides a close simulation of the physical processes in a full-scale utility boiler. The arrangement of the major components of our slipstream system are shown in Figure 1. Flue gas extracted from the main duct of the CCF passes through a spray/steam tower to establish the desired temperature and relative humidity conditions. The Fabric Filter Sampling System (FFSS) draws about 2.5 acfm of flue gas from this conditioned stream. The remainder of the flow passes through the ESP and a venturi, and into the main pulse-jet baghouse used to provide particle collection for the CCF. The CCF is operated so the pressure drop between points where we access the CCF process stream induces the desired flow of 280 acfm through the ESP.

Flue gas enters at the top of acylindrical spray tower to condition the flue gas stream. The chamber is 10 ft tall and has a diameter of 36 inches. Residence time in the chamber is approximately 18 seconds. We can inject a fine spray of water droplets or dry steam into the chamber to add moisture to the flue gas. After leaving the chamber the flue gas enters a transform to the ESP. The slipstream ESP is a relatively small, single field, single flow passage unit, and is < 90 % efficient. These factors should aid in our characterizations of reentrainment. The ESP's single flow passage has six 1/8-inch diameter wires in series. Plate-to-plate spacing is nine inches. Each plate can be rapped with up to 100 g force. The ESP is equipped with windows on the inlet and outlet transforms. At our target flow of 280 acfm the ESP has a specific collection area (SCA) of about 62 ft^2/kacfm.

The FFSS is used to simulate operation of a fabric filter with reverse-gas cleaning. The FFSS draws flue gas isokinetically from the transform immediately upstream of the ESP. We placed an absolute filter in parallel with the FFSS filtration cabinet to periodically measure the total mass entering the device. The filtration cabinet is independently maintained at our target temperatures. Operating temperatures, flows and filtering pressure drop are output to the data acquisition system.

We have installed continuous monitors (Environmental Systems Corporation model P-5A) upstream and downstream of the ESP to measure total mass concentrations in the flue gas. This instrument collects and measures back-scattered light from fly ash particles entrained in the flue gas. Because accurate assessments of temperature and relative humidity are critical to the interpretation of the FFSS and ESP data, we are monitoring these parameters very closely. Thermocouples are located at critical

points throughout the system, and relative humidity has been assessed by direct measurement of the water content of the flue gas, and with a continuous monitor located just upstream of the ESP. A computer utilizing Labtech Notebook® software acquires and stores data for our system. This data acquisition system displays and records temperatures, flow rates, FFSS pressure drops, and ESP inlet and outlet mass concentrations. Values from all monitors connected to the data acquisition system are sampled every 2 seconds and a snapshot value is recorded to a data file every 30 seconds.

Besides coal type, flue gas temperature and water content are primary independent variables in our test matrix. Therefore we closely monitor the temperature and relative humidity in the FFSS and ESP. We can use a combination of water spray, steam injection, and passive heat exchange (removing insulation from ducts) to bring the flue gas to the desired levels of temperature and humidity.

The CCF flue gas normally contains about 8 % water by volume. Therefore the normal relative humidity in the 300 °F flue gas we are extracting from the CCF duct has been around 1.7 %. Initially, for each CCF test, we plan to characterize baseline operation of the ESP and FFSS at this condition. Our laboratory data and our review of field experiences indicate that the most likely conditions for electrostatic reentrainment are high relative humidity and relatively cool flue gas. We also expect that the strongest liquid bridges that we can form in the dust cake in the FFSS will result from relatively moist conditions. During each of the CCF's standard runs, the pilot-scale combustor is run at full load for two consecutive 24-hour test periods. Depending on the time it takes to condition the ash layer on the ESP plates, we can test three to five conditions overall during each CCF test run.

We have used two different means for identifying the onset of electrostatic reentrainment. Because the ESP we are using has windows at both ends that allow illumination and viewing of the wires and plates, we have been able to visually inspect the collected ash layer on the plates as the conditions in the ESP are varied. We also have observed the output of our outlet continuous mass monitor as we attempted to induce reentrainment. We plan to measure the size distribution of samples of dust cake ash collected in the FFSS. After each test, we will obtain ash samples from various points in the ESP process stream. The laboratory tests we plan to perform on these samples include tensile strength, uncompacted bulk porosity, size distribution, true particle density, resistivity, and chemical analysis. When we have isolated conditions in the ESP that promote reentrainment, these tests should help us determine if this reentrainment is due solely to flue gas conditions, or if the characteristics of the particles were altered by conditioning.

Results

At the time of this writing, we have participated in two CCF tests. The first test was performed in December 1993, and lasted for about 240 hours. During this test, we exercised the system (except for the conditioning chamber, which was not ready for operation at that time) and evaluated the baseline operation of the ESP and FFSS. The key operating parameters we examined included temperature loss through the ESP and associated ductwork, V-I characteristics of the ESP, rapping procedures for the ESP, buildup of properly conditioned ash layers on the ESP collection plates and the FFSS fabric, rate of ash accumulation in the ESP and FFSS hoppers, length of FFSS cleaning cycles, degree of air in-leakage, maintenance and stability of flue gas flow rates, mass concentrations in the flue gas, flue gas moisture content, operation and sensitivity of the continuous mass monitor, sample collection, and collection of data with our automated data acquisition system. Our continuous mass monitor served as a reliable indicator of relative changes in mass concentrations in the outlet duct.

The second of our pilot-scale combustor tests was performed during January 1994. The primary objectives of this test were to assess the effects that humidification and cooling had on the characteristic gas flow resistance of a dust cake collected in a fabric filter, and on the reentrainment of particles from ash layers collected in an ESP. We used a fine spray of water droplets to moisten and cool the flue gas and condition the fly ash particles in the conditioning chamber. The glass windows located at the inlet and outlet of the ESP were used to observe ash levels in the hopper and the effects

of rapping on the ash layers accumulated on the ESPs grounded collection plates. In order to rapidly collect ash layers on the ESP plates, we rapped the plates only after evaluating a particular combination of flue gas temperature and moisture. During our first test, we measured mass concentration downstream of the ESP with the voltage on and off. (Time limitations precluded the measurement of mass concentraion during the second test.) Without the cooling induced by the water spray, the temperature at the inlet of the ESP was about 292 °F. Flue gas temperature dropped by about 8 to 10 °F through the length of the ESP. During our first test we operated the ESP with a current density between 30 and 40 nA/cm^2.

We used woven fiberglass fabric with a 25% exposed surface texturization for our filtration substrate. This is fabric commonly used at utility reverse-gas baghouses. Since one of our primary objectives was to establish a cleaning schedule that would provide fast, accurate assessment of the pressure drop characteristics of the ash, we operated the FFSS with 1 and 2 hour filtering cycles. Because the calculation of K_2 requires knowledge of the rate of accumulation of ash on the fabric, we used the rate of pressure drop accumulation at a constant flow rate as our parameter for evaluation of ash filtration characteristics during our first test. For our second test, we measured the mass concentration entering the FFSS by placing a mass train thimble in parallel with the FFSS. This allowed us to normalize the rate of pressure drop increase by the mass concentration entering the FFSS. (The mass of ash reaching the filter cake cannot be directly measured because of the near-continuous operation of the FFSS, and the influence that the geometry of the FFSS transform has on selective particle settling.)

During our second CCF test, the ESP was operated with a current density of about 30 nA/cm^2. (Periodically during our tests we measured V-I curves for the ESP. We maintained the applied voltage between 38 and 43 kV to build ash layers on the grounded plates. At these voltages, the current density ranged from 2.5 to 33 nA/cm^2.) We maintained relatively stable operation at about 290 °F for about 6 hours and collected a relatively thick ash layer on the ESP plates. We then began conditioning with water spray to cool the ESP inlet to around 168 °F. While the flue gas and slipstream ducting were cooling, we also lowered the set points on the FFSS ovens and probe heaters to around 165 °F. After temperatures stabilized, we operated the ESP and the FFSS for several hours. We then began to increase the temperature in the ESP by reducing the volume of water spray. We discontinued FFSS operation during the period of transition in flue gas temperature. Severe reentrainment from the ESP plates was observed at an ESP inlet temperature of about 193 °F. We reestablished stable ESP and FFSS operation at about 220 °F. This episode of reentrainment can be seen in Figure 2.

From an ESP operating temperature of around 220 °F, we gradually lowered the flue gas and ESP temperature to around 165 °F by increasing the water spray. However, during this drop in temperature, we were not able to reproduce the reentrainment phenomenon we observed during the temperature rise through 193 °F. We then cleaned the ESP plates and re-deposited an ash layer at an operating temperature of about 165 °F. The FFSS was also brought back on line at this temperature and allowed to operate for four hours. During this period, the filtering pressure drop across the fabric in the FFSS did not increase. Our experiences at other operating temperatures would tend to attribute much of this inability to build pressure drop to a decrease in the fundamental gas flow resistance (K_2) of the filter cake. However, even a much lower K_2 should still result in a gradual increase in filtering pressure drop. We also measured lower mass concentrations at the inlet to the FFSS at this temperature, but we would still predict some increase in pressure loss through the fabric.

After an ash layer had been formed in the ESP at 165 °F, we isolated the FFSS and began a ramp up in temperature. We observed severe reentrainment at ESP inlet temperatures between 198 and 218 °F (Figure 2). After cleaning the ESP plates and reheating the system to around 260 °F, we maintained stable operation of the FFSS at this temperature. After operation at 260 °F, we once again attempted to induce reentrainment by gradually decreasing operating temperatures. We did observe an increase in emissions from the ESP at about 203 °F. Unfortunately, this event coincided with a soot blow in the CCF, and we cannot be certain the emissions we saw were due to reentrainment from the ESP. Visual observations through the ESP window did show significant amounts of ash falling off the plate

during this period; however, similar reentrainment was often viewed through the window when no significant increases in outlet emissions were being measured by the P5-A.

We once again dropped the system temperature to about 165 °F and built a new ash layer on the ESP plates. We then gradually increased the system temperature and again observed highly active reentrainment of the collected ash. This time the reentrainment occurred at an ESP inlet temperature of about 182 to 187 °F. During this episode of reentrainment the relative humidity in the ESP was about 16 %. We continued to increase system temperature all the way up to about 220 °F, but we did not observe additional significant reentrainment. We then reheated the system to about 272 °F to obtain more FFSS operating data. We also rebuilt ash layers on the ESP plates at this temperature. As we had done before, we attempted to induce reentrainment of these ash layers by gradually dropping system temperature with water spray injection. No significant reentrainment was observed as we slowly lowered the system temperature to 150 °F. However, when we raised the temperature of the inlet to the ESP back up to around 203 °F, we again observed the reentrainment phenomenon.

Observations from FFSS Operation. In order to analyze the effects that duct humidification had on the filtration characteristics of the ash collected in the FFSS, we observed two main parameters: the rate of pressure drop increase across the filtering fabric, and the amount of ash entering the FFSS filtration cabinet. These data are summarized in Table 1. The final column in this table normalizes the rate of pressure drop increase by the mass concentration we measured with the mass train thimble we placed in parallel with the FFSS. This normalized value should provide a fair indication of relative changes in K_2 at different flue gas conditions. The relative humidity values presented in Table 1 were calculated from moisture determinations performed on samples taken from the ESP outlet duct during the corresponding FFSS test periods. The values in Table 1 indicate that rate of pressure drop increase falls as humidity increases. (The data obtained at around 260 °F vary from this trend.) For a more definite assessment of this effect, we will obtain more FFSS data between 300 and 165 °F during subsequent tests. Although we will be performing more evaluations during later CCF tests, we have shown that this type of conditioning was able to reduce filtering pressure drop.

Observations from ESP Operation. In order to evaluate the ability of flue gas humidity and temperature to affect the electrostatic reentrainment of deposited layers, we observed the ash layers and the performance of the ESP as we slowly increased or decreased the flue gas temperature. We altered temperature by varying the amount of water injected into the conditioning chamber. Several factors may have complicated our observations. Our visual observations of the ash layers deposited on the ESP plates indicated that the appearance of the layer depended on the relative humidity in the ESP during deposition. When ash layers were deposited at around 275 °F (1.2 % RH) the ash layer looked smooth, with many large craters in its surface. In contrast, the ash layers deposited under high humidity conditions (22 % RH at about 165 °F) appeared fluffy, and the surface of the layer seemed to be composed of small (1/32 inch diameter) agglomerates of ash particles. This appearance agrees with the kind of fluffy structures we observed in laboratory measurements of uncompacted bulk porosity at relatively high humidities. We would expect that these fluffy ash layers have a higher porosity and probably a different tensile strength than the smooth layers formed at lower relative humidities. Since the major reentrainment phenomena we observed were from these fluffy ash layers, the characteristics (porosity and tensile strength) of the layer may be key factors in inducing reentrainment.

Because the temperature and humidity of the flue gas were changing as we approached conditions where reentrainment was likely (around 190 °F and 18 % RH), the ash layers on the ESP plates were either drying out or adsorbing additional moisture as the ESP passed through the conditions most conducive to reentrainment. The actual water content of the ash layer may not have been the same during ascending and descending temperature conditions. Ash resistivity is a key factor in the reentrainment phenomenon. Resistivity is strongly influenced by adsorbed water on the ash, as well as by ash temperature. Therefore the same factors that may have affected the porosity and tensile strength of the ash layer, may also have significantly influenced ash resistivity.

The ash we saw being ejected from the ash layers on the plates usually came off as small (~1/8 inch) chunks. Visual observation could not determine what became of the chunks after they fell into the gas stream. Since the bulk cohesivities of the ash layers formed at high and low relative humidities are probably quite different, the chunks of ash that we observed reentering the flue gas stream from the ash layers may have behaved differently in the inter-electrode region. In the laboratory, we observed the decrepitation, or breaking up, of agglomerates of ash lofted into the inter-electrode space in the electrostatic tensiometer we used to measure tensile strength. If the degree of difference in cohesivity was sufficient to induce or prevent significant decrepitation of the chunks of ash entrained from the ash layer, then we may actually have been inducing reentrainment during our descending-temperature transitions. The reentrained chunks of ash may have been too cohesive to decrepitate, and therefore may have fallen rather quickly and directly into the ESP hopper. This type of reentrainment would have been visible through the ESP window, but would not have been detected by our continuous mass monitor. On the other hand, the fluffier chunks of ash formed at high humidities may have decrepitated more fully, and led to the large increases in outlet emissions sensed by our P5-A monitor.

Large deposits formed on the discharge electrodes during operation at low temperatures and high humidities. The deposits were about 1 inch wide transverse to flow and up to 4 1/2 inches long in the direction of gas flow. The deposits formed at higher temperatures and lower humidities were only about 1/8 inch thick and were more radially symmetrical. We are not sure what effects these buildups have on reentrainment (besides an alteration of field strength required to obtain a given total current).

ACKNOWLEDGMENTS

This work was sponsored by the U.S. Department of Energy, Pittsburgh Energy Technology Center under Contract No. DE-AC22-91PC90365. Mr. Tom Brown has recently taken over as Project Manager from Ms. Felixa Eskey.

REFERENCES

1. T. Gillespie, "The Contribution of Electrostatic Induction to the Long Range Forces between Solid Particles," Particulate and Multiphase Processes, 3: 3-10 (1987).
2. S.J. Rothenberg, "Coal Combustion Fly Ash Characterization: Adsorption of Nitrogen and Water," Atmospheric Environment, 14(4): 445-456 (1980).
3. M.C. Coelho and N. Harnby, "The Effect of Humidity on the Form of Water Retention in a Powder," Powder Technology, 20(2): 197-200 (1978).
4. E.C. Landham *et al*, "Effects of Spray Dryer Effluent on the Performance of the Laramie River Unit 3 ESP," presented at the Ninth Particulate Control Symposium, Williamsburg, VA, October 15-18, 1991.

Table 1
Summary of FFSS Operation

FFSS orifice temperature, °F	approximate RH in FFSS, %	Δ(Fabric ΔP)/hr, in. H_2O/ hr	FFSS inlet mass concentration, gr/acf	Δ(Fabric ΔP)/hr/FFSS inlet mass concentration, (in. H_2O/ hr)/gr/acf
300	1.3	0.23	1.15	0.20
300	1.3	0.22	1.15	0.20
300	1.2	0.40	1.65	0.24
260	2.5	0.30	1.03	0.29
220	6.1	0.11	0.75	0.14
190	--	0.00	--	--
165	22	0.01	0.38	0.02
165	23	0.01	0.45	0.02

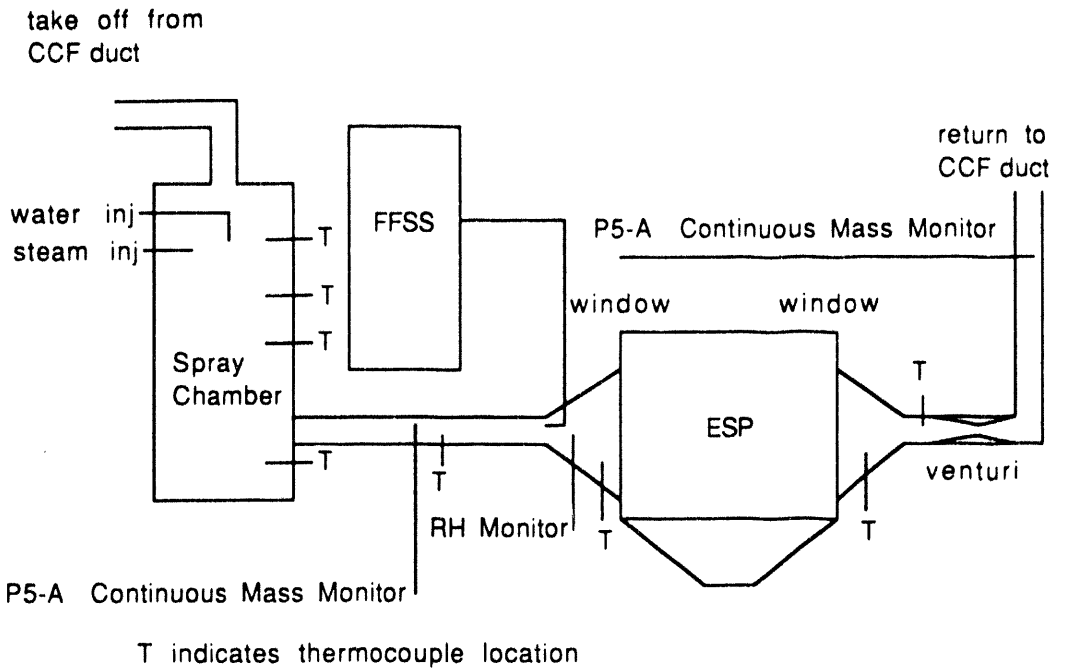

Figure 1. Schematic diagram showing the major components of our pilot-scale test setup.

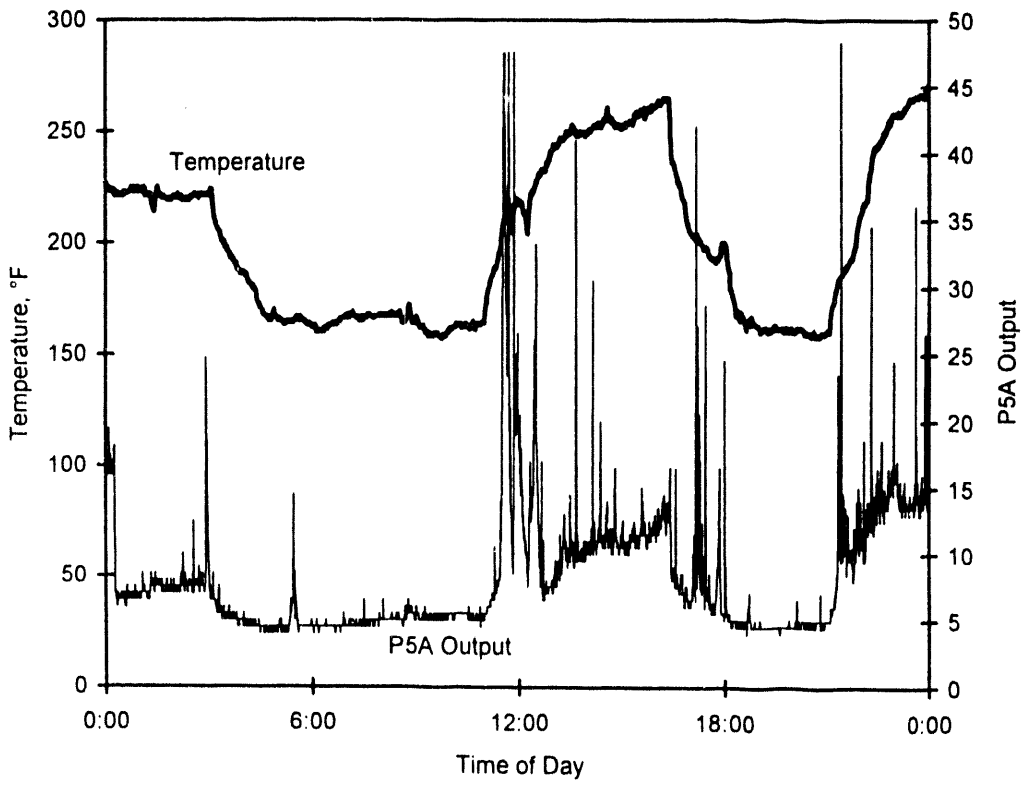

Figure 2. Comparisons of ESP inlet temperature and P5-A outlet monitor output. Visually verified reentrainment events correspond to periods when the ESP temperature was being increased.

BENCH-SCALE AND PILOT-PLANT EVALUATION OF ADDITIVES FOR IMPROVED PARTICLE COLLECTION IN ELECTROSTATIC PRECIPITATORS

MICHAEL DURHAM, PH.D., KEN BALDREY,
TIMOTHY EBNER, RICHARD SCHLAGER, AND SHARON SJOSTROM
ADA TECHNOLOGIES, INC.

I. Introduction

The purpose of this research program is to identify and evaluate additives capable of increasing particle cohesion to improve collection efficiency in an ESP. Flue gas conditioning that changes the cohesive characteristics of the particles has the potential to improve collection efficiency because a large percentage of particulate emissions from a well-performing ESP is due to reentrainment. Improved ESP performance should result if particle reentrainment could be reduced by making the particles "stickier" or more adhesive. This could produce a significant reduction in emissions from an ESP from the following mechanisms:

- o Reduced erosion-type reentrainment
- o Reduced rapping emissions
- o Reduced hopper reentrainment
- o Increased agglomeration of fine particles

A flue gas conditioning system would have several advantages as a retrofit technology for improving the collection efficiency of ESPs. Conditioning is cost effective because it requires no modifications to the ESP. Current flue gas conditioning systems are relatively simple and can be applied to almost any ESP and installation requires minimal downtime of the boiler. Finally, it could also be used on new ESP designs to provide high collection efficiency with a reduced collection area.

A three-phase screening process is being used to provide the evaluation of many additives in a logical and cost-effective manner. The three-step approach involves the following experimental setups:

1. Provide a preliminary screening in the laboratory by measuring the effects of various conditioning agents on reentrainment of flyash particles at simulated flue gas conditions.
2. Evaluate the successful additives using a 100 acfm bench-scale ESP operating on actual flue gas.
3. Obtain the data required for scaling up the technology by testing two or three of the most promising conditioning agents at the pilot scale.

These test programs will be supplemented by separate analytical tasks to study the surface properties of the additives, to extrapolate experimental data using a computer ESP model, to characterize the waste, and to determine the costs for a full-scale flue gas conditioning system.

The selection of additives and the initial screening of the additives in the laboratory are described in Durham et al., 1993. This paper describes the results of the bench-scale and initial pilot-scale testing of the most promising additives.

II. Bench-Scale ESP Testing

Bench-scale testing was conducted at the Consolidation Coal Company Research and Development Laboratory in Library, PA. Flue gas from the CONSOL pilot combustor duct was drawn through an isokinetic probe assembly, into an injection chamber where the conditioning agents were introduced, through ADA's bench-scale ESP, and then through a flow measuring venturi by the system's ID fan. The flue gas exiting the ID fan was returned to the combustor. A sketch of the arrangement is shown in Figure 1.

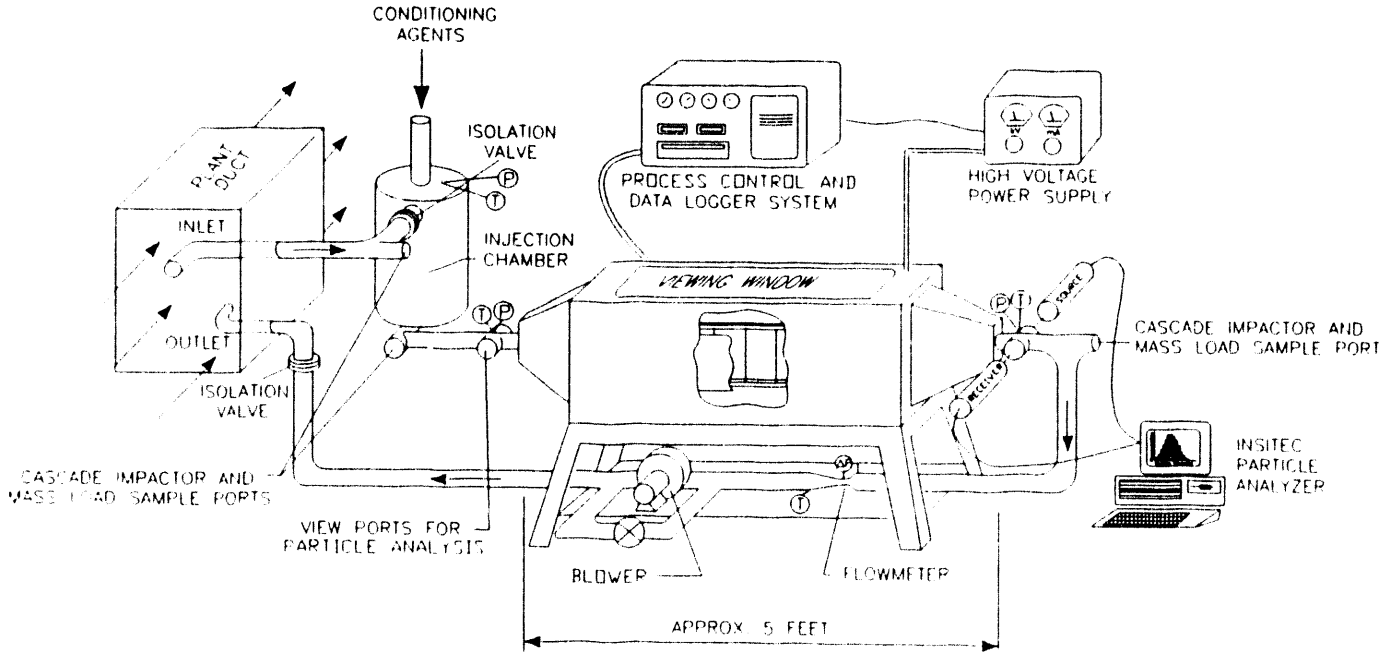

Figure 1. Bench-Scale ESP Configuration

A. Residence Chamber and Additive Injection

The residence chamber was sized to provide a nominal residence time of 2 seconds for 100 acfm of flue gas. The chamber consisted of a 12 inch diameter, 4 foot high cylindrical vessel with co-current mixing of additive and flue gas. Flue gas entered the heated chamber tangentially near the top of the vessel and spiraled to the perpendicular exit located near the chamber's base. The additive was injected through a nozzle mounted to the upper blind flange on the residence chamber.

The additive was metered to the injection nozzle using a peristaltic pump. The initial calibration indicated that the accuracy of the pump was within $\pm 1\%$ for the desired additive flow rate range (3 to 10 cc/min). The injection nozzle was a dual fluid nozzle which required air to produce the desired additive spray pattern. The air pressure was manually controlled and monitored with the other system flow and pressure parameters.

B. Bench-Scale ESP

The ADA portable bench-scale ESP was sized for a nominal 100 acfm using 12 inch high, 36 inch long plates which can be installed at various plate-to-plate spacings. For these tests, five plates were spaced 2.25 inches apart to form 4 gas passages and to provide an SCA of 240 ft^2/Kacfm. The discharge electrodes are supported by a rigid frame. The electrodes are 0.1" diameter wires spaced 4 inches apart. A high voltage power supply was sized to allow operation up to 25 Kv and 5 mA. At full capacity with the ESP arrangement at CONSOL, the power supply could potentially produce a field strength of 8.75 kV/cm and a current density of 224.3 nA/cm^2.

The ESP was heated and insulated to control and maintain a constant operating temperature. The system can be operated from ambient to 400°F. The ESP collector plates were manually rapped from outside the box. The plate hanger at the outlet end of the ESP was connected to a rod which extended through the top of the box. A ratchet mechanism was incorporated to lift the back end of the plates approximately 1/2 inch and drop them back on their mounts.

III. Bench-Scale Results

The bench-scale ESP was installed at the CONSOL combustion research and development facility in order to evaluate the additives while precipitating flyash from an actual coal-fired boiler. During a two-week test, four candidate additives were injected into the flue gas ahead of the 100 acfm ESP to determine the effect on fly ash collectability.

For each additive, the tests were conducted by first operating at baseline conditions with no additives and then repeating the test with additives. In order to produce the identical gas stream characteristics under both baseline and additive conditions, the injection nozzle was operated for both cases. During baseline testing with no additive injection, a 0.5 cc/min feed of clean water was injected through the nozzle into the chamber. A 250 ml flask acted as the

liquid reservoir to the peristaltic pump. To start an additive injection test, a 250 ml flask containing an additive concentration was exchanged with the baseline water flask. At the completion of an additives injection test, the process was reversed and a second baseline measurement was performed.

During an initial 5 hour test, additive "C" was injected at varying rates over a five hour period. A rate was chosen for the main testing based upon preliminary economic studies and positive results from the initial test. The short initial test did not provide enough data to confidently predict the effect of differing injection rates. Furthermore, due to time constraints, the injection rate was not optimized during the bench-scale testing. Injection rates for additives "A", "B", and "D" were chosen to be economically comparable to additive "C".

Table 1 shows a summary of the results of the additives tests during both weeks of testing. Additive "A" was found to pose operational problems for the ESP almost immediately. The ESP began sparking and outlet particle loadings increased from baseline levels by an average of 8%. Additive "B" was found to slightly decrease the outlet particle loading by 2% as compared to the baseline conditions. Additive "C" improved collection efficiency from 40% to 50% during the first week of testing, and from 65% to 74% during the second week after additional baffles were installed in the ESP. This represents a reduction in emissions of 17% and 27%. Additive "D" was also found to be effective by reducing outlet mass loadings 17% as compared to baseline (no additive) conditions.

Table 1. Summary of Bench-Scale Testing

Test Date	Test Condition	Collection Efficiency	Particle Penetration	Emission Reduction	Test Temperature
5/13	Baseline	40.4%	59.6%		307°F
5/13	Additive C	50.4%	49.6%	16.8%	308°F
5/14	Baseline	34.4%	65.5%		305°F
5/14	Additive A	28.9%	71.1%	-8.5%	307°F
5/14	Baseline	42.8%	57.2%		300°F
5/14	Additive B	44.1%	55.9%	2.3%	305°F
5/14	Additive D	52.4%	47.6%	16.8%	287°F
5/19	Baseline	64.6%	35.4%		308°F
5/19	Additive C	74.3%	25.7%	27.4%	307°F

Particle size distribution measurements were made using an InSitec Laser Particle Analyzer. These measurement demonstrated that the additive causes a significant and fairly uniform decrease in emissions for particles below 10 micrometers in diameter, which is the range of accuracy for the Insitec.

IV. Pilot Plant Testing

The two conditioning agents that performed successfully in the bench-scale tests were evaluated using a pilot-scale ESP. These tests were conducted at the Consol Combustion Facility in Library, PA. The pilot-scale test program extended for two weeks during September and October, 1993. During the tests, the research combustor was firing a medium-sulfur coal. The combustor had recently been retrofitted with low-NOx burners for a DOE Clean Coal test program. Operation of the low-NOx burners required a reduced flow rate in the combustor, resulting in lower flow and velocity in the ESP.

During the first week, a comprehensive baseline condition was tested, followed by initial screening runs for several additives. It was discovered that at the conditions tested, the flyash exhibited properties characteristic of a high-resistivity ash. In-situ measurements at the ESP inlet confirmed that the resistivity was in the 10^{10} - 10^{12} ohm-cm range. In addition, the ESP plate rappers were not able to remove ash buildup on the first section during normal operation. Power off rapping was periodically required to fully clean the plates; this is a clear indication of high-resistivity conditions.

Since the major benefit of ESP additives will be to reduce reentrainment at low to midrange resistivity, this operating condition was undesirable for performance testing. It was decided to continue the program with SO_3 conditioning of the flue gas to reduce particle resistivity. It was also decided to operate with two rather than three electrical fields energized. By reducing the ESP collection area, it was hoped that it would be easier to measure changes in ESP performance and to see an immediate indication of the effectiveness of SO_3 conditioning.

During the second test week, the ESP was reconfigured with two electrical sections energized and SO_3 conditioning at a rate of approximately 20 ppm. An additional baseline test was run, followed by extended tests with two additives, referred to in this report as additive 'C' and additive 'D'. The system was allowed to return to baseline at the conclusion of the tests.

The CONSOL research combustor and ESP are extensively instrumented and can be configured for a variety of operating conditions. For the baseline test, the electrical sections were combined to give a 3 field configuration. Gas velocity in the precipitator was 1.7 ft/sec, based on a measured inlet flow rate of 468 acfm. Specific collection area (SCA) at this condition was 204 ft^2/kacfm. The precipitator was operated in a current limited mode throughout the test period. For the second week of testing, two electrical sections were energized. Gas velocity and flow rate in the precipitator were unchanged from the baseline. SCA was 129 ft^2/kacfm.

Voltage, current, and power for each electrical section were monitored continuously. Particulate buildup on the plates was also monitored via load cell transducers. Opacity was monitored at the ESP outlet, using a transmissometer mounted along a straight section of the outlet duct, for improved resolution. System temperatures, flow rates, and gas constituents exiting the boiler were also monitored.

Additive Injection

Additive was introduced to the flue gas via a fine spray nozzle oriented upstream in the duct at a point downstream of the combustor convection zone outlet approximately 60 ft. upstream of the ESP. The ducting has several sharp bends between the spray point and the ESP, which ensured good contact between additive and entrained particulate prior to the ESP. Duct velocity was 22 - 25 ft/sec immediately upstream of the ESP inlet cone.

The spray nozzle had been previously calibrated at ADA's Nozzle Test Facility and was found to produce an extremely fine mist of approximately 10 μm droplet size. This results in an additive droplet which is an order of magnitude smaller. Injection rate was controlled using a peristaltic pump with pressure regulated compressed air. Actual consumption of additive solution was also monitored gravimetrically.

V. Pilot Plant Results

The pilot-scale tests indicate that ESP performance decreased during the additive injection period. However, it is unclear if the performance decrease was due to the effect of the additives or to an unrelated shift in ESP baseline operation. The opacity decreased somewhat during the final baseline condition, but the ESP did not fully recover to the initial Week 2 baseline.

ESP operating conditions during the initial pilot-scale tests were not well-matched to the target conditions where increased particle adhesion could have a beneficial effect on ESP performance. High resistivity meant that reentrainment was already minimal and little, if any, improvement would be expected. If the additives were further increasing particle cohesion and contributing to plate surface buildup, in a high resistivity situation, the ash layer would be even harder to remove, potentially decreasing performance. Thus, it is possible that the additives were performing as anticipated, but were simply not in the correct operating regime. Examination of Fields 2 and 3 load cell data during Week 2 of testing shows steadily increasing ash layer buildup which periodic rapping did not remove.

The only conclusive way to determine additive effectiveness will be to test under conditions where non-rapping reentrainment seriously decreases ESP performance, in the range of 10^7 to 10^9 ohm-cm ash resistivity. The electrostatic forces are relatively flat in this range, so that changes in flue gas conditions that will result in a change in resistivity by up to two orders of magnitude will have little effect on the magnitude of reentrainment. Also, at the very low resistivity conditions, reentrainment will be the highest and performance improvements will be easier to measure.

VI. Conclusions

A variety of additives were evaluated relative to their ability to increase the cohesive characteristics of flyash. Laboratory and bench-scale tests have identified several additives that improved the performance of ESPs and fabric filters leading to lower particulate

emissions. The most successful candidates are non-toxic, as they are used in foods and cosmetic products. Preliminary chemical analysis of conditioned fly ash shows that it passes the Toxicity Characteristic Leaching Procedure criteria.

In addition, the chemicals are relative inexpensive. A preliminary economic analysis was performed to evaluate the cost of the additive process and to compare its costs against alternative means for reducing emissions from ESPs. The results show that conditioning with additive C at a rate of 0.05% (wt. additive to wt. fly ash) is much less expensive than adding new ESP capacity, and more cost competitive than existing chemical conditioning processes that may not be nearly as effective. Table 2 compares the complete levelized costs (over a 30-year plant life) of the cheapest chemical at various feed rates and its associated capital and O&M requirements to the other proprietary process.

Table 2. Levelized Cost Of Injection Process Using Chemical C At Various Feed Rates

	Proprietary Process	Chemical C @ 0.1%	Chemical C @0.05%
Chemical Cost	$35,300/mo*	$1.90/lb+	$1.90/lb+
$/ton Coal	0.50●	0.39♦	0.36♦

* Monthly cost of chemical and equipment lease. Does not include escalation over 30-year plant life.
\+ Current cost per pound of highly refined chemical.
● Does not include escalation over 30-year plant life.
♦ Levelized cost over 30-year plant life.

NON-TOXIC ADDITIVES FOR IMPROVED FABRIC FILTER PERFORMANCE

JEAN BUSTARD, GEORGE CRATER, TIMOTHY EBNER,
SHARON SJOSTROM, AND RICK SLYE
ADA TECHNOLOGIES, INC.

Introduction

The overall objective of this Phase I Small Business Innovation Research (SBIR) program was to demonstrate the feasibility of using non-toxic additive products as flue-gas conditioning agents for the improvement of particulate air toxics control and overall fabric filter performance. Current flue-gas conditioning agents such as SO_3/NH_3 have successfully improved fabric filter performance by reducing both particulate emissions and tube sheet pressure drop (Miller and Laudal, 1993); however, there are health, safety, and hazardous waste issues associated with them. Conditioning agents that would provide an alternative to SO_3/NH_3 were identified for evaluation in this program. Additive products were chosen that:

- Would potentially increase particle cohesion,
- Are not currently used as flue-gas conditioning agents,
- Are non-toxic, and
- Are cost competitive.

Eleven new additives were evaluated in this laboratory test program. Four additives were identified as potential non-toxic conditioning agents that reduced outlet emissions by at least 90% compared with baseline conditions. This paper describes the test fixture, approach and results from these tests.

Experimental Apparatus

Testing was conducted in ADA's laboratories. The test apparatus consisted of a 1) flue-gas simulator to control both gaseous and particulate matter concentrations, 2) an additive injection system, 3) a filter test device to monitor fabric filtering properties and performance over time, and 4) a continuous particle monitor. Figure 1 presents a sketch of the laboratory test set-up.

Flue-gas Simulator

A laboratory flue-gas simulator was used to provide a 6 acfm flow of gas. The flue-gas was heated and controlled to a temperature of 350°F. Dry gas phase constituents (NO, SO_2, and CO_2) were mixed and regulated using mass flow controllers and introduced into the heater/oven assembly. The required N_2 and O_2 concentrations of the gas stream were produced through the dilution of room air with bottled N_2. This N_2-O_2 mixture was then passed through a temperature controlled water bath/bubbler to produce the necessary H_2O vapor concentration. The humidified N_2-O_2 mixture was conveyed through heated sample

lines to the heater/oven assembly, where it was then mixed with the other gas constituents. The heated gas mixture was then seeded with flyash from a screw feeder that meters the dust into an eductor. The simulated flue-gas mixture was then introduced into the top of the injection chamber, where the candidate gas conditioning agents were added. Flue-gas simulator settings are established by an electronic spreadsheet that calculates individual mass flow controller settings, water bath temperature, and gas volume (cylinder pressure) required to meet specified operating conditions.

Additive Injection Chamber

The additive injection chamber was designed for a minimum residence time of two seconds for flowing flue-gas. The chamber was 4 inches in diameter and 16 inches long. The simulated flue-gas stream entered the chamber tangentially. The additives were injected in a water solution at one end of the chamber at very low rates using a dual fluid atomizing nozzle. With this nozzle, complete evaporation of the injected liquid occurred in the additive chamber, as there was no evidence of wall wetting or solids deposits in the main body of the injection chamber.

Filter Test Device

Fabric filter performance was evaluated in ADA's Filter Test Device (FTD). The FTD can be configured as either a pulse-jet or a reverse-gas fabric filter, or can be modified to test other filter designs such as ceramic filters. In this test it was configured as a pulse-jet fabric filter with short segments of full-size bags and used a cleaning system that was designed to simulate fabric cleaning forces typically associated with full-scale installations. A microprocessor-based datalogger is incorporated into the FTD control panel, which combines precision measurement capability with processing and control functions in a single, battery-operated system. The datalogger monitored temperatures throughout the system, along with tubesheet pressure drop, pulse pressure, cleaning pulse rate, flow rate, and outlet emissions.

Continuous Particle Monitor

A Triboflow^{TM} dust monitor was installed in the outlet ductwork of the FTD for continuous, real-time monitoring of outlet particle concentration. The Triboflow^{TM} sensor was chosen for this study because it is very sensitive to small changes in particle concentration, as each particle that impacts the probe produces a change in electrical current. In addition, a test port was located downstream of the Triboflow^{TM} for EPA Method 17 mass tests.

Test Procedures

Additives were selected that would potentially increase particle cohesion. Eleven additives were identified by drawing on results from a DOE/PETC research program on flue-gas conditioning for electrostatic precipitators and experience with the causes of desirable and undesirable dust cake characteristics. A few of the key additive properties in this selection process were: 1) behaviors that could induce "stickiness" and thus enhance agglomeration, 2)

compounds that imparted no toxic or hazardous properties to the ash, and 3) compounds that could be handled simply for injection into the flue-gas.

The laboratory test fixture was used to conduct the performance evaluation tests of the additives. The goal of these tests was to determine if each additive produced a beneficial, detrimental, or negligible effect on filtration performance. An economic analysis was then performed for the most promising additives. The test sequence followed a 3-step process:

1. Perform initial screening of additives.
2. Optimize injection rates for candidate additives.
3. Conduct a longer-term performance test on each candidate additive.

Screening Tests

An initial set of screening tests were conducted to choose the most promising additives from the entire suite of potential additives. Each additive was mixed with distilled water to obtain the target additive-to-ash mass ratio. Baseline conditions (lignite coal flyash injected at a rate of 10 gr/acf, gas flow rate of 6 acfm, water injection at 1 cc/min, and an operating temperature of 350°F) were established before additive injection was begun. The system was then operated with each additive until the FTD had passed through five cleaning cycles or until a significant change in performance was documented. The system was returned to baseline immediately following an additive test to document whether fabric filter performance returned to baseline values.

Optimization

A second series of tests were conducted on the most promising additives to optimize the concentration of additive required to produce beneficial effects. Additives were mixed and injected several additive-to-ash ratios. The solutions were injected sequentially from lowest to highest concentration until the Triboflow™ sensor indicated that the outlet emissions had been reduced by a factor of 10. These concentrations were chosen for further testing.

Longer-Term Tests

Following the optimization tests, a series of longer-term performance tests were conducted to confirm initial screening results, to gather longer-term performance data, and to conduct EPA Method 17 mass concentration tests to verify Triboflow™ data. Prior to each test, a new woven fiberglass bag was installed. The bag was conditioned overnight at baseline conditions. Two modified EPA Method 17 mass tests were conducted at the outlet of the fabric filter after operation at baseline conditions for at least 8 hours. Additive injection was then begun and the fabric filter operated with additives for at least 1 hour before an additional series of three modified EPA Method 17 mass tests were begun. The FTD was operated for nominally 8 hours with each additive.

Upon completion of the longer-term tests with the candidate additives, the FTD was operated with SO_3/NH_3 to compare the effects of these flue-gas conditioning agents with those

of the candidate additives. This final test was conducted using the same procedure as the performance tests, except that only the Triboflow™ was used to monitor outlet emissions.

Results

Screening Tests

The Triboflow™ sensor was used as the primary, real-time indicator of the effectiveness of an additive during the initial screening tests and the optimization tests. Table 1 shows the average Triboflow™ output signals for each of the 11 additives screened and the corresponding baseline level. The change in outlet emissions due to additive injection varied from an increase of 6% over baseline to a decrease of 94%. The Triboflow™ sensor responded almost immediately, by showing a signal drop of at least an order of magnitude upon injection of four of the additives. These additives were numbers 6, 7, 9 and 10. These four were chosen for additional testing.

Optimization Tests

The Triboflow™ sensor output was monitored in strip-chart format on the test system computer. This was particularly useful during the optimization tests. After a baseline was established, injection of the lowest additive-to-ash concentration level was begun. Injection of the next higher additive concentration was begun when it was established that no significant change had occurred. Optimized injection rates varied by a factor of 10.

Longer-Term Tests

The longer-term performance tests verified the results from the initial screening tests, as measured by both the Triboflow™ sensor and modified EPA Method 17 mass tests. Table 2 shows the results of the Method 17 tests and the resulting calculated reduction in outlet emissions. The baseline outlet particle loadings were repeatable and uniform, as shown in the table. The outlet loadings during additive injection are also quite uniform, which indicate that the additive concentrations chosen during the optimization tests produce a repeatable, similar affect on the dustcake. Figure 2 shows the TriboFlow™ response to the injection of each of the four candidate additives. In each case, the signal drops immediately after additive injection is initiated.

A linear regression of the results from the Triboflow™ output and the EPA Method 17 mass test results resulted in a correlation coefficient is 0.95, demonstrating that the Triboflow™ was an excellent indicator of total particle mass exiting the fabric filter in this test.

The additives had a negligible effect on cleaning frequency or pressure drop. The FTD was set-up to clean when the tube sheet pressure drop reached 5.0 inches H_2O. The time between cleans for the four additive tests and the corresponding baseline tests are shown in Table 3. This phenomenon will be evaluated further in future tests, as it was expected that a

reduction in either pulse cleaning frequency or tube sheet pressure drop would have occurred with both the new additives and the SO_3/NH_3.

The traditional flue-gas conditioning combination of NH_3 and SO_3 was evaluated in the laboratory test fixture to compare the response of the system to SO_3/NH_3 and the new additives. Figure 3 compares the effect on outlet emissions due to injection of additive 7 and SO_3/NH_3. The graph on the left shows that the outlet emissions dropped from 7% to less than 0.5% when additive #7 was injected at a concentration of 0.25% of the mass of flyash in the flue gas. The graph on the right shows an almost identical effect on the outlet emissions when a mixture of SO_3 and NH_3 was injected at 18 ppm SO_3 and 36 ppm NH_3.

Economic Analysis

An economic analysis showed that an injection system for the four most promising additives can be installed and operated at levelized costs that are one-half to one-sixth the cost of an SO_3/NH_3 system. The savings can be conservatively estimated at 1 mill per kWhr.

Conclusions

Tests were performed on eleven new, non-toxic flue-gas additives in a lab-scale system to demonstrate the feasibility of using novel products as flue-gas conditioning agents for the improvement of particle emissions and overall fabric filter performance. Four additives were identified as, cost effective candidates for continued evaluation.

In April continued funding for this program was awarded as a SBIR Phase II grant. The overall objective of the Phase II program is to demonstrate that the candidate additives are successful at a larger scale on flue-gas from a operating coal-fired boiler.

References

Miller, S.J., and D.J. Laudal (1993). "Pulse-Jet Baghouse Performance Improvement". Presented at the Ninth Annual Coal Preparation, Utilization, and Environmental Control Contractors Conference, Pittsburgh, PA, July 19-22.

Table 1. Results of Additive Screening Tests.

Additive	Baseline Signal	Additive Signal	Emission Reduction (%)
#2	12.0	8.4	30
#3	11.0	8.1	26
#4	9.0	8.5	5
#5	8.5	4.5	47
#6	8.8	0.7	92
#7	7.2	0.7	90
#8	9.4	7.9	16
#9	10.3	0.7	93
#10	7.7	0.5	94
#11	8.2	8.7	(6)
#12	8.7	7.5	14

Table 2. Outlet Emissions During Longer-term Tests.

Additive	Baseline (gr/dscf)	Additive (gr/dscf)	% Reduction in Emissions
#6	0.262	0.016	94
#7	0.262	0.021	92
#9	0.292	0.026	91
#10	0.287	0.026	91

Table 3. Cleaning Frequency During Longer-Term Testing.

	Time Between Cleans (min)	
Additive	Baseline	Additive
#6	54	59
#7	60	57
#9	61	62
#10	97	111

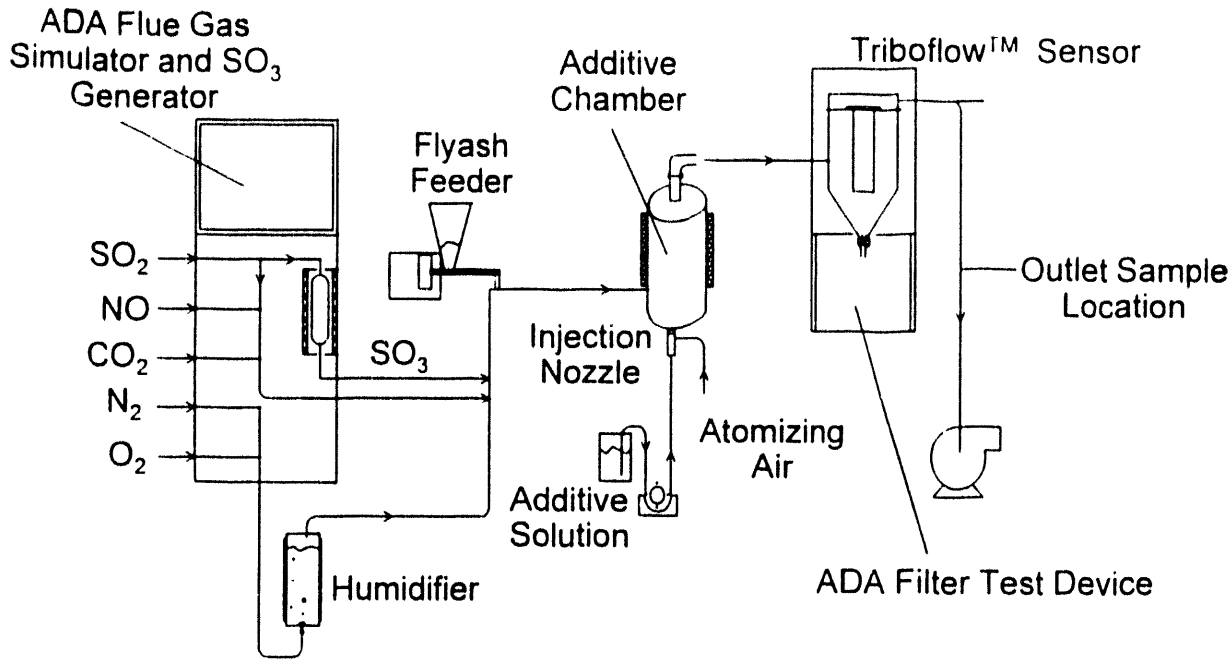

Figure 1. Schematic of Phase I Test Apparatus

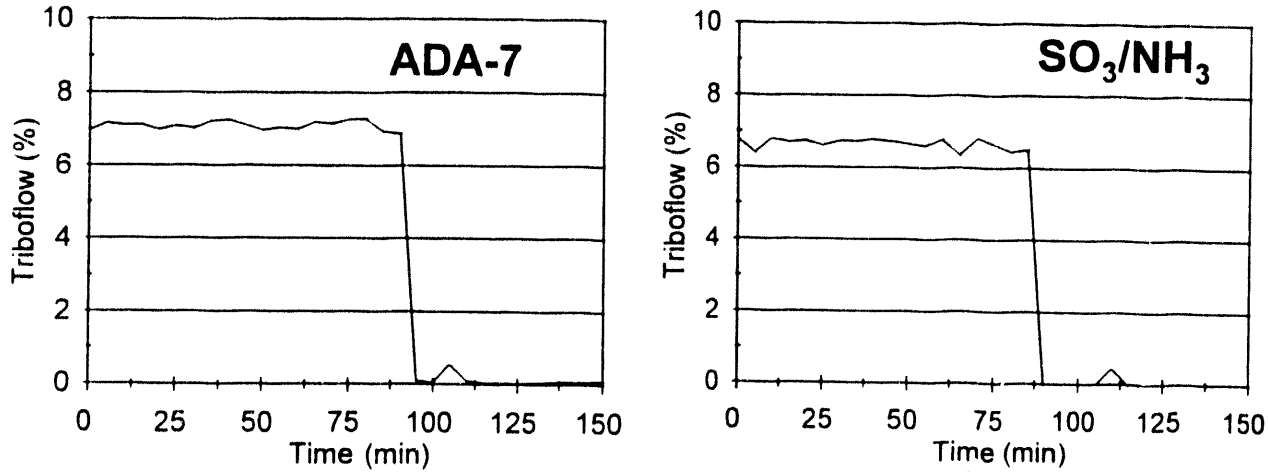

Figure 3. Comparison of Triboflow™ output recorded during additive 7 test and SO_3/NH_3 test.

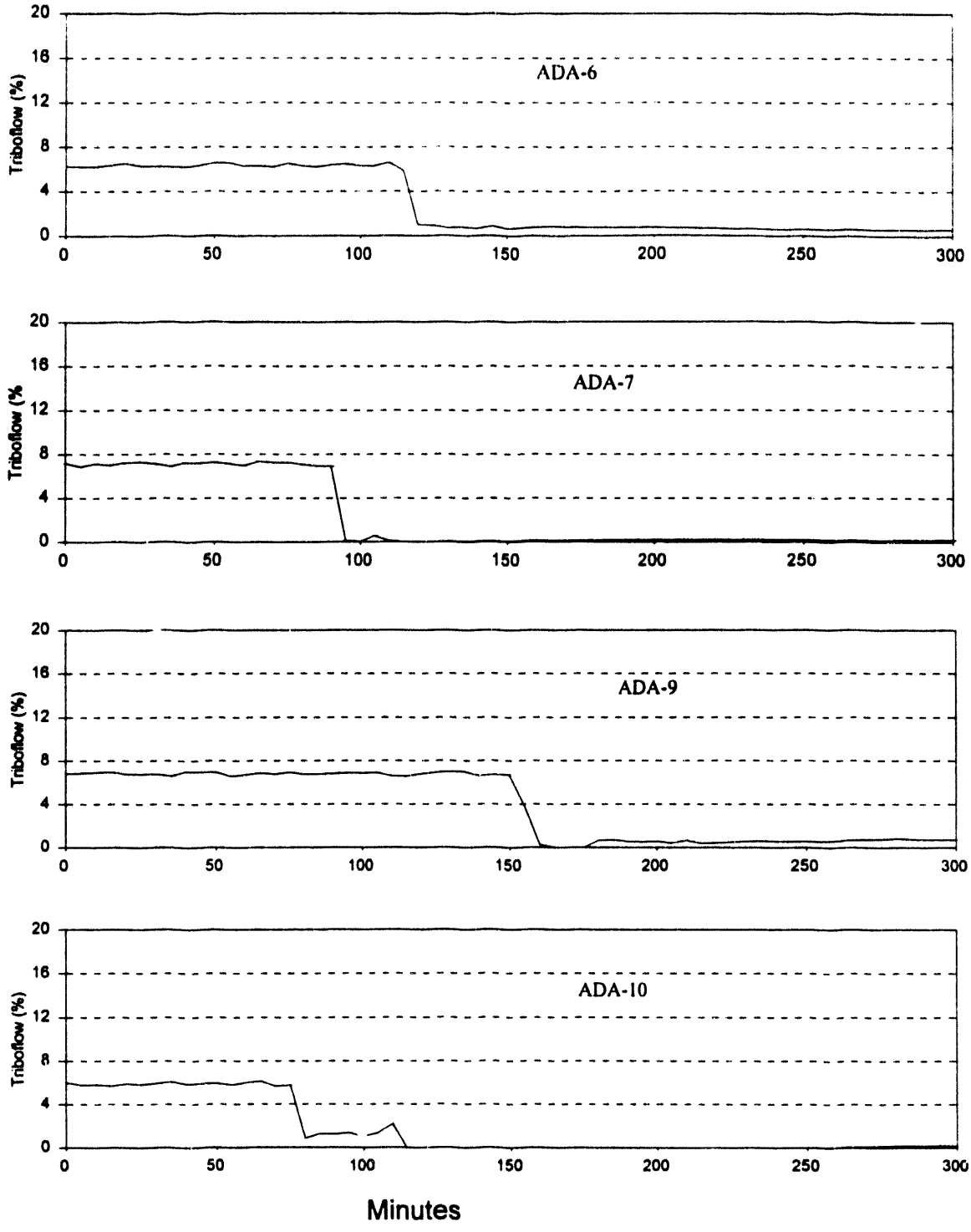

Figure 2. Triboflow^{TM} response to the injection of each of the four candidate additives.

CATALYTIC FABRIC FILTRATION FOR SIMULTANEOUS NO_x AND PARTICULATE CONTROL

GREG F. WEBER, PROJECT MANAGER
GRANT E. DUNHAM, RESEARCH ENGINEER
DENNIS L. LAUDAL, RESEARCH ENGINEER
SUMITRA R. NESS, RESEARCH ENGINEER
GRANT L. SCHELKOPH, RESEARCH ENGINEER
ENERGY & ENVIRONMENTAL RESEARCH CENTER
UNIVERSITY OF NORTH DAKOTA
PO BOX 9018
GRAND FORKS, ND 58202-9018

OBJECTIVE

The University of North Dakota Energy & Environmental Research Center (EERC); Owens-Corning Fiberglas Corporation (OCF); and Raytheon Engineers & Constructors (RE&C), conducted research to develop a catalytic fabric filter for simultaneous NO_x and particulate control. Funding for the project was provided by the U.S. Department of Energy/Pittsburgh Energy Technology Center (DOE/PETC), Consolidated Edison Company of New York Inc. (Con Edison), and the Empire State Electric Energy Research Corporation (ESEERCO). OCF provided catalyst-coated bags, fabric samples, and technical support as a cost share. The DOE/PETC program is intended to demonstrate technology showing significant advances in the state of the art using a process or a combination of processes capable of reducing NO_x emissions to 60 ppm or less. Other requirements include that a nonhazardous waste or a salable by-product be produced and that the concept be applicable to both new and retrofit coal-fired systems. A potential for a 50% cost savings must also be demonstrated in comparison to a commercial selective catalytic reduction (SCR) process capable of meeting the 60-ppm NO_x emission limit.

Advances at OCF showed that a high-activity catalyst can be applied to a high-temperature woven glass cloth, resulting in a fabric filter material that can operate at temperatures higher than the maximum operating temperatures of commercially available coated glass fabric. The NO_x is removed by catalytic reduction with ammonia to form nitrogen and water. The catalyst employed at this time is vanadium-titanium, but the exact catalyst composition and the unique method of applying the catalyst to high-temperature glass fabric are the property of OCF (1). Other catalyst options are being evaluated by OCF in order to improve catalyst performance and minimize the cost of catalyst-coated bags.

Bench-scale experimental results have shown that over 90% NO_x removal can be achieved and that the catalyst/fabric has promising self-abrasion characteristics (2, 3). However, development of the technology required further evaluation of air-to-cloth ratio effects, ammonia slip, SO_2 oxidation to SO_3, temperature cycling, catalyst-coated fabric preparation, fuel impacts, fabric cleaning (reverse-gas versus pulse-jet), catalyst life (poisoning and resistance to erosion), and filter life and performance (particulate control, differential pressure, and durability).

ACCOMPLISHMENTS AND CONCLUSIONS

Process Testing Pulse-Jet Baghouse System

A 500-hr pulse-jet test was completed in December 1992. The purpose of the 500-hr test was to determine the effectiveness of a catalyst-coated fabric filter to control particulate and nitric oxide

emissions simultaneously. Three coal-fired experimental periods were planned in order to address the effect of ammonia/NO_x molar ratio (0.8 [twice] and 0.9) at a constant air-to-cloth ratio of 3 ft/min. Baghouse temperature was nominally 650°F, and flue gas was generated by firing a Blacksville bituminous coal in a pilot-scale pulverized coal (pc)-fired combustor. Blacksville bituminous coal is characterized by low moisture (1.7 wt%) and moderate ash (8 wt%) and sulfur (2.3 wt%) content. Sieve analysis indicated that the pulverized coal averaged 76 wt% -200 mesh. The coal ash analysis showed high levels of silica, alumina, and iron as oxides and low alkali levels. These values represent the average of three composite samples, one taken each week of operation.

Eight pulse-jet filter bags (6 in. in diameter by roughly 8.25 ft long) supplied by OCF were used for this test. The filter bags were prepared using a high-temperature woven glass consisting of D-fibers (6.5-micron) having a fabric weight of 22 oz/yd^2. Seven coats of a vanadium-titanium catalyst were applied to the fabric using an organic-based coating process. This is the same fabric type used during four previous 100-hr pulse-jet tests (4). The 500-hr pulse-jet test began with heat treatment of the catalyst-coated bags. This consisted of a 2.5-hr heatup period, during which the baghouse temperature was raised from roughly 417° to 716°F, followed by a 4-hr heat treatment period at 720°F and 3.3% oxygen to remove a fugitive lubricant used in the bag manufacturing process. The flue gas for heat treatment was generated by firing natural gas.

Figure 1 presents the NO_x removal efficiency and ammonia slip (% of inlet NO_x) as a function of ammonia/NO_x molar ratio for all of the coal-fired test periods. The first week at a nominal ammonia/NO_x molar ratio of 0.8, daily average NO_x reduction ranged from 78% to 83%. The average baghouse bulk gas temperature was 658°F, and the inlet NO_x concentration averaged 946 ppm. Ammonia slip concentrations ranged from 1.0% to 7.6% (9 to 70 ppm) of inlet NO_x concentration and increased on the average over the week.

During the second week of coal firing, the ammonia/NO_x molar ratio was nominally 0.9, and average daily NO_x reduction ranged from 81% to 87%. The average baghouse bulk gas temperature was 659°F, and the inlet NO_x concentration averaged 953 ppm. Ammonia slip concentrations ranged from 9.0% to 17.0% (86 to 157 ppm) of the inlet NO_x concentration.

During the third week, the nominal ammonia/NO_x molar ratio was 0.8. The average daily NO_x reduction ranged from 76% to 83%. The average baghouse bulk gas temperature was 659°F, and the inlet NO_x concentration averaged 941 ppm. The ammonia slip concentrations ranged from 5.9% to 8.6% (50 to 85 ppm) of the inlet NO_x concentration.

Before the 500-hr test was terminated, short coal-fired test periods at nominal ammonia/NO_x molar ratios of 0.6, 0.7, and 0.8 were completed. At an average ammonia/NO_x molar ratio of 0.64, NO_x reduction averaged 62%. Ammonia slip concentrations were 1.5% (13 ppm) of the inlet NO_x concentration. At an ammonia/NO_x molar ratio of 0.71, NO_x reduction averaged 69%. Ammonia slip concentrations were 2.6% (24 ppm) of the inlet NO_x concentration. Two short test periods at ammonia/NO_x molar ratios of 0.77 and 0.87 were also completed before system operation was terminated. The NO_x reduction averaged 74% during the first test period and 80% during the second test period. The ammonia slip concentrations were 4.0% and 7.2% (37 and 68 ppm) of the inlet NO_x concentration.

In general, the overall performance of the bags was good, indicating that 80% NO_x reduction was possible with an ammonia slip of 7.5% of the inlet NO_x concentration when injecting ammonia at a molar ratio of 0.85. Although an apparent decrease in catalyst reactivity occurred during the first week of operation, as evidenced by the increased ammonia slip, catalyst performance appeared stable during the second and third weeks.

Sulfur trioxide (SO_3) measurements were made with ammonia injection turned off, and the concentrations ranged from 1.0 to 6.0 ppm, all less than 1% of the flue gas SO_2 concentration. Sulfur

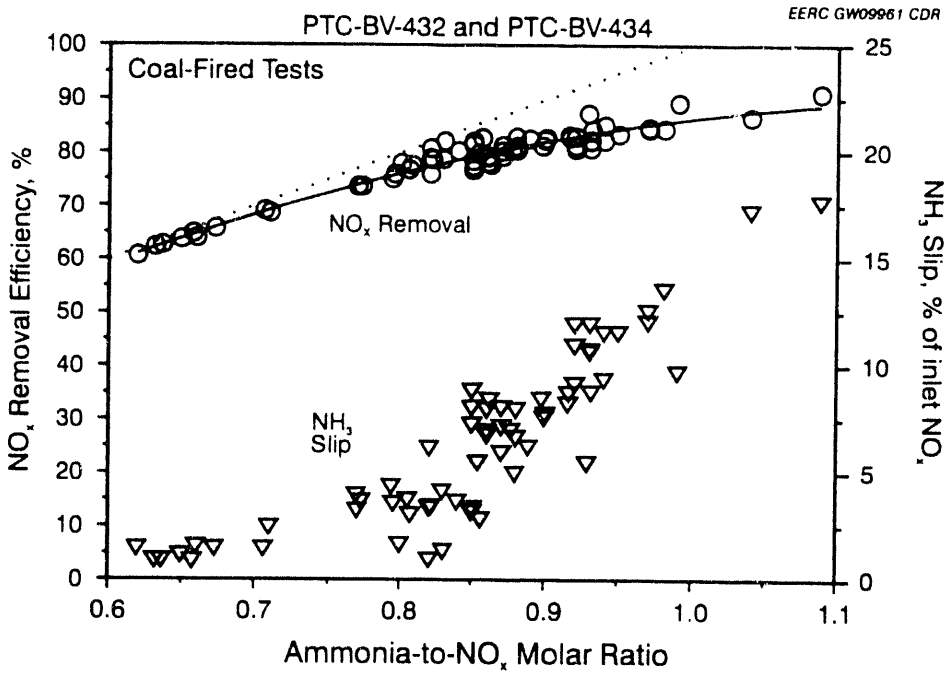

Figure 1. NO_x removal efficiency as a function of ammonia/NO_x molar ratio, 500-hr coal-fired tests.

dioxide concentration was relatively constant (1500 to 1700 ppm) and the SO_3 data gave no indication of decreasing catalyst reactivity with time.

Pressure drop and particulate emissions data were also collected during the 500-hr test. Particulate emissions measurements were made using a modified EPA Method 5, a multicyclone, and an aerodynamic particle sizer (APS). Integrated averages of respirable mass were taken during APS sampling on 6 individual days with the ammonia injection turned off. The respirable mass integrated averages ranged from 0.06 mg/m^3 to 1.1 mg/m^3 and, with the exception of one data point, indicated that emissions decreased with time. The exception to the trend represents a sampling period during which bag cleaning was frequent and not representative of baghouse performance during the 500-hr test period. Respirable mass emission concentrations reported here are similar to values reported elsewhere for pulse-jet baghouse operation with conventional fabric types (woven glass and Ryton) (5).

Particulate emissions were well below 0.03 lb/MMBtu when the ammonia injection was off and only approached 0.03 lb/MMBtu when ammonia slip was greater than 40 ppm. Values approaching 0.03 lb/MMBtu that occurred during ammonia injection periods are believed to result from the formation of ammonium sulfates and bisulfates in the sample system. However, in a commercial system, ammonium sulfates and bisulfates formed as a result of ammonia slip would primarily deposit in the air heater, resulting in little or no effect on measured particulate emissions.

Particulate collection efficiency during the 500-hr test averaged 99.61% and ranged from 99.36% to 99.91% with the ammonia injection turned on, representing emissions ranging from 0.0021 to 0.0134 gr/scf. With the ammonia injection turned off, particulate collection efficiency averaged 99.96% and ranged from 99.89% to 99.99%, representing emissions ranging from 0.0003 to 0.0034 gr/scf. Particulate sampling data indicated that the inlet mass loading to the filters averaged about 2.0 gr/scf. After completion of the 500-hr test, there was little dust on the tube sheet, and the bags appeared to be in good shape.

The pulse-jet bags were cleaned as a function of baghouse differential pressure. Initially, the cleaning cycle trigger point was 5 in. W.C., and the pulse-air reservoir pressure was 60 psig. However, during the first part of the third week of operation, the bags were cleaning every 30 minutes and, occasionally, off-line. At this point, the cleaning cycle trigger point was increased to 6 in. W.C., and the pulse-air reservoir pressure remained at 60 psig. After the change in trigger point, the time between bag cleanings increased to every 90 min. Figure 2 plots the baghouse pressure drop as a function of time for the 500-hr test. Data presented in the figure show that baghouse ΔP, after cleaning, increased with time until the trigger point was increased from 5 to 6 in. W.C. From that point on, baghouse ΔP after cleaning was relatively stable at 3 to 4 in. W.C.

A concern with the use of catalyst-coated bags is the possibility of catalyst erosion resulting in decreased NO_x reduction, increased ammonia slip, and an increase in the vanadium content of the fly ash. Although vanadium is not a Resource Conservation and Recovery Act (RCRA) element, some vanadium compounds are considered hazardous materials. Therefore, it is important to monitor vanadium concentration in the fly ash in order to determine if catalyst is lost from the fabric.

Vanadium concentrations on various new fabric samples representative of those used during the 500-hr test ranged from 6230 to 7160 μg/g. Based on the analysis of fabric samples collected from one bag, no vanadium catalyst was lost from the pulse-jet bags used during the 500-hr pulse-jet test. Measured vanadium concentrations ranged from 6440 to 6760 μg/g. The data also indicate that there is a 5% to 10% variation in vanadium concentration on the fabric surface for a single bag. Analysis of coal and ash samples supports the conclusion that vanadium loss from the catalyst-coated fabric was not observed as a result of the 500-hr test.

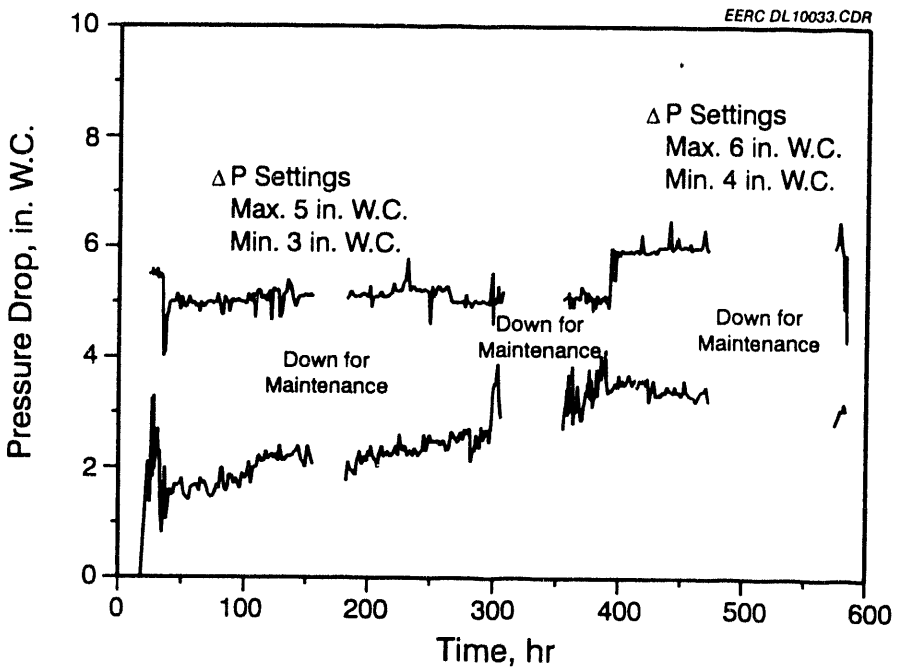

Figure 2. Baghouse differential pressure as a function of time.

Fabric Durability Testing/Pulse-Jet System

The purpose of this activity was to evaluate the durability of the catalyst-coated fabric in a pulse-jet system filtering flue gas as a function of time with on-line cleaning. Baghouse operating conditions were monitored on a continuous basis and particulate emissions were measured monthly. Ammonia injection was not used and NO_x concentration measurements were not made. Changes in catalyst reactivity were determined as a result of bench-scale NO_x reduction tests using fabric samples cut from bags removed from the baghouse at specified intervals.

The slipstream baghouse at the University of North Dakota Steam Plant had accumulated 5136 hours when operation was terminated in December 1993. The baghouse contained nine bags in a 3 x 3 array roughly 6 in. in diameter by 8 ft long. Average flue gas temperature ranged from 500° to 650°F at an air-to-cloth ratio of 3 to 5 ft/min and a baghouse differential pressure of nominally 2 to 4 in. W.C., with a few excursions in the 6- to 8-in. W.C. range. Supplemental ash injection was used to augment the particulate mass loading from the stoker-fired boiler. The resulting baghouse inlet mass loading was roughly 1.5 to 5.7 gr/scf. The injection ash used represented material collected from the baghouse hoppers of pilot-scale pc-fired and circulating fluid-bed combustors. The chemical composition of the ash represented a wide range of ash types–bituminous, subbituminous, and lignite ash as well as CFB ash containing a large amount of calcium present primarily as sulfate and free oxide.

Particulate collection efficiency was measured on a monthly basis. Results of the particulate sampling completed showed particulate collection efficiency ranging from 99.96% to >99.99%. Measured outlet emissions ranged from 0.0001 to 0.0011 gr/scf. Using the APS sampling system, the respirable mass emissions were found to be low, averaging <0.1 mg/m^3.

Multicyclone sampling indicated that on a mass basis, 74%–97% of the fly ash entering the baghouse had an aerodynamic diameter >10 microns. Sampling at the outlet of the baghouse showed a sulfur trioxide (SO_3) concentration of <1 ppm. Moisture, oxygen, and carbon dioxide concentrations in the flue gas were observed to be 4% to 8%, 8% to 13%, and 7% to 12%, respectively.

Catalyst-coated DE992 bags were removed from the slipstream baghouse periodically to determine fabric strength and catalyst reactivity as a function of flue gas exposure. Bags were removed at 840, 1642, and 5136 hours. Physical characterization of the three bags by OCF personnel focused on fabric strength and endurance. Fabric strength was measured using the Mullen burst test. Figure 3 presents data for the Mullen burst test in a bar graph format. Each bar represents an average value for five fabric samples tested and indicates a standard deviation. The data indicate that fabric strength, as determined by the Mullen burst data, increased with increasing hours of exposure to flue gas. Average burst pressures for the fabric exposed to flue gas for 840, 1642, and 5136 hours were 618, 660, and 739 psig, respectively. Standard deviations ranged from 35 psig to 90 psig. No explanation has been found to explain the apparent increase in fabric strength as a function of flue gas exposure.

Fabric endurance was determined using the MIT flex or folding endurance test. Again five samples from each bag were tested with the results presented in Figure 3. The data indicate that there was no change in fabric strength, as determined by the MIT flex test, with increasing hours of flue gas exposure. Average cycles to failure ranged from 488 to 505, with standard deviations ranging from 55 to 100 cycles to failure.

Catalyst-coated fabric samples were also cut from the bags removed from the slipstream baghouse in order to perform bench-scale catalyst reactivity tests. Reactor temperature was 650°F , the filter face velocity was 4 ft/min, and the inlet NO_x concentration was 725 ppm. The results showed that variability in the data for multiple samples from a single bag was typically less than 2% NO_x reduction, and closure on the ammonia was typically 97% to 103%. Fabric samples tested from the three bags removed from the slipstream baghouse at the UND Steam Plant demonstrated NO_x reduction (75% at an ammonia/NO_x molar ratio of 0.8) and ammonia slip (<5% of the inlet NO_x concentration) levels similar

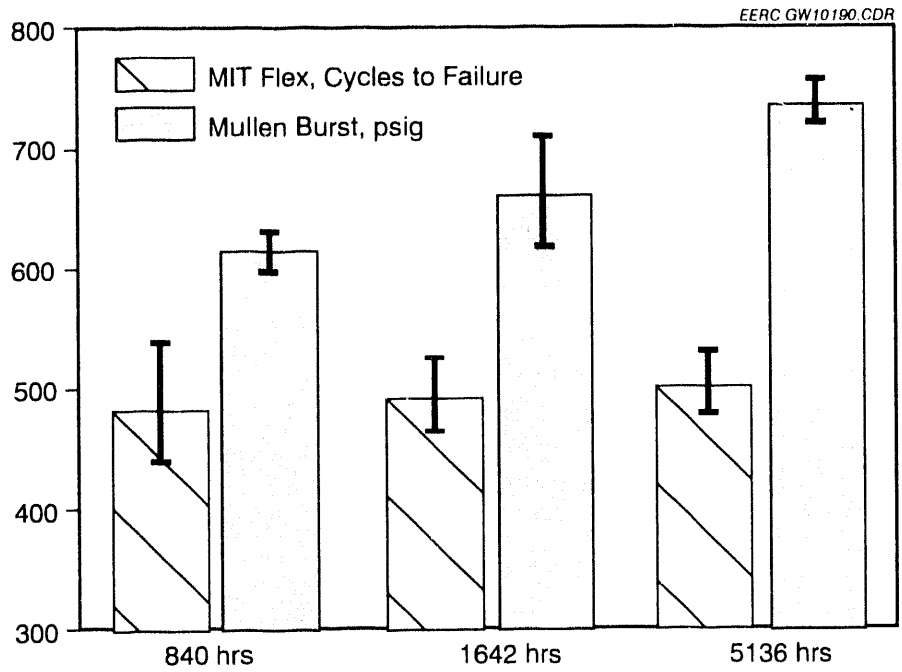

Figure 3. Mullen burst and MIT flex test data for three catalyst-coated bags versus flue gas exposure times of 840, 1642, and 5136 hours.

to those observed for fabric samples removed from bags used during the 500-hr test. Therefore, the exposure of the DE992 catalyst-coated bags to flue gas in the slipstream baghouse at the UND Steam Plant did not have any detrimental effects on fabric strength or catalyst reactivity for over 5000 hours of flue gas exposure.

CONCEPTUAL DESIGN AND ECONOMIC EVALUATION

To determine the commercialization potential of the catalytic fabric filtration (CFF) concept, RE&C was asked to develop a conceptual design and prepare an economic evaluation of the CFF process to estimate capital, operating, and levelized costs for two commercial pc-fired boiler applications, a new 500-MW plant and an older 250-MW plant. In both cases, the CFF concept was compared to conventional hot-side SCR for NO_x control and cold-side pulse-jet fabric filtration (PJFF) for particulate control. The economic analysis was prepared based on Electric Power Research Institute (EPRI) technical assessment guidelines (TAG) (6). Results from the experimental activities were used as a basis for system design with respect to process conditions such as CFF face velocity. In both cases the evaluation assumed that NO_x concentrations exiting the boilers had been minimized as a result of combustion controls, low-NO_x burners. The conceptual design and economic evaluation effort was completed by RE&C under subcontract to the EERC and documented in a report summarizing the assumptions and results (7).

The economic evaluation showed that the total installed plant investment for the CFF concept was 5% higher than the total installed plant investment for the SCR/PJFF combination, $145/kW versus $138/kW, for the new 500-MW plant and 4% lower for the 250-MW plant, $213/kW versus $221/kW.

On a levelized cost basis, the CFF concept was somewhat less costly than the SCR/PJFF system for the new 500-MW plant, 5.91 versus 6.33 mills/kWh, and for the 250-MW retrofit, 9.15 versus

10.07 mills/kWh. Levelized costs for the CFF are driven by catalyst-coated bag replacement costs. Elements driving levelized costs for the SCR/PJFF included SCR catalyst replacement costs and the additional ID fan power requirements to offset pressure losses across the SCR reactors and the PJFF.

Cost sensitivity analysis for the CFF showed that the cost of the catalyst-coated bags has the strongest effect on overall economics, capital and levelized costs, for the 500-MW new plant and the 250-MW retrofit.

The conceptual design and economic evaluation completed by RE&C indicates that the CFF is economically competitive with the SCR/PJFF, but further CFF development is necessary in order to compete commercially with the better developed technologies. Therefore, future CFF development efforts must focus on reducing the cost of catalyst-coated bags, demonstrating a bag and catalyst life of >2 years, and improving performance with respect to NO_x reduction and ammonia slip at air-to-cloth ratios equivalent to or higher than those used in this evaluation.

PLANS

As of the presentation of this paper, all of the experimental and reporting activities planned in the original scope of work have been completed. Results from the project have been summarized in a final report (8). The Catalytic Fabric Filtration project contract terminates on August 31, 1994.

REFERENCES

1. Kalinowski, M.R.; Nishioka, G.M. "Method for Applying Porous Metal Oxide Coatings to Relatively Nonporous Fibrous Substrates," U.S. Patent 4 732 879, March 22, 1988.

2. Weber, G.F.; Laudal, D.L. "SO_x/NO_x Control - Catalytic Fabric Filtration for Simultaneous NO_x and Particulate Control," final technical report for the period Apr. 1, 1988, through Jun. 30, 1989; DE-FC21-86MC10637, EERC publication, Aug. 1989.

3. Weber, G.F.; Miller, S.J.; Laudal, D.L. "Flue Gas Cleanup," final technical report for the period July 1, 1989, through June 30, 1990; DE-FC21-86MC10637, EERC publication, Oct. 1990.

4. Weber, G.F.; Ness, S.R.; Laudal, D.L.; Dunham, G. "Catalytic Fabric Filtration for Simultaneous NO_x and Particulate Control,; quarterly technical progress report for the period July 1 - Sept. 30, 1992; DE-AC22-90PC90361, EERC publication, Oct. 1990.

5. Miller, S.J.; Laudal, D.L. "Pulse-Jet Baghouse Performance Improvement with Flue Gas Conditioning," final project report; Prepared for EPRI and U.S. DOE, Oct. 1992.

6. Electric Power Research Institute. "Technical Assessment Guide: Volume 1: Electric Supply 1989," EPRI Report No. p-6587-L, Revision 6, Sept. 1989.

7. Raytheon Engineers & Constructors. "Catalytic Fabric Filter Technology for the Simultaneous Control of NO_x and Particulate Emissions from Coal-Fired Boilers," Task 4 Conceptual Engineering and Economic Evaluation; prepared for the Energy & Environmental Research Center, Oct. 1993.

8. Weber, G.F.; Dunham, G.E.; Laudal, D.L.; Ness, S.R.; Schelkoph, G.L. "Catalytic Fabric Filtration for Simultaneous NO_x and Particulate Control," final report prepared for the U.S. Department of Energy Pittsburgh Energy Technology Center, Contract No. DE-AC22-90PC90361; EERC publication, April 1994.

HOLLOW FIBER CONTACTORS FOR SIMULTANEOUS SO_X/NO_X REMOVAL

Abhoyjit S. Bhown
Dean B. Alvarado
Neeraj R. Pakala
Susanna Ventura
SRI International
333 Ravenswood Avenue
Menlo Park, CA 94025

Kamalesh K. Sirkar
Sudipto Majumdar
Debabrata Bhaumik
New Jersey Institute of Technology
University Heights
Newark, NJ 07102

DOE Contract No. DE-AC22-92PC91344
Period of Performance: 5/1/92 to 4/30/97

INTRODUCTION

Control of SO_X and NO_X emissions from coal-fired utility and industrial boilers is a topic of growing national and international importance. Whereas a host of commercial and semi-commercial processes exist (Drummond and Gyorke, 1986), increasingly stringent emission standards mandate that processes be low cost, highly efficient, and, ideally, produce marketable byproducts. Although a wide range of site-specific economic factors dictate the best choice of SO_X and NO_X control, removal of SO_2 by wet limestone scrubbing and removal of NO_X by selective catalytic reduction (SCR) are regarded as the best commercialized technologies for this application. A typical wet limestone plant requires approximately \$100 to \$120 of capital investment per kilowatt of electric power generating capacity and has power and miscellaneous operating costs in the range of 5 to 6 mils per kilowatt hour (kWh). The SCR process requires approximately \$70 to \$100 of capital investment per kilowatt of electric power generating capacity. Its operating costs, including ammonia consumption, is in the range of 1.8 to 2.2 mils per kWh. These costs can add approximately 20% to the final cost of generated electricity, a significant burden on rate payers.

Our proposed research is aimed at developing (to a subscale prototype size) a new process for removal of SO_X and NO_X that is more than 20% less costly than limestone scrubbing of SO_2 and selective catalytic reduction of NO_X, removes at least 95% of the SO_X and 75% of the NO_X, and produces salable byproducts with no waste material. To accomplish this objective, we intend to develop a regenerable wet scrubbing process for SO_X and NO_X that exploits the advantages of a class of novel contacting devices, known as hollow fiber contactors (HFC), and that uses novel SO_X and NO_X absorption chemistry. The HFC devices will bring substantial capital cost savings to our process. The novel use of the contactors for regenerating the SO_2 scrubbing liquor and the novel NO_X absorption chemistry will help reduce the energy consumption.

This development program will include three phases conducted over 60 months. The initial phase, encompassing the first 24 months of the project, will emphasize demonstrating the technical feasibility of each component of the flue gas control process—including process chemistry, mass transfer rates, and the ability of the HFC modules to function in the presence of particulate matter. At the end of this phase, we expect to have demonstrated 99% SO_2 removal efficiency and 85% NO_X removal efficiency in the laboratory. These efficiency targets are greater than the final goals of this project. The second phase of the work is designed to develop scale-up rules for the HFC modules and to test the longevity of the NO_X scrubbing chemistry. In the 15 months of this second phase, we expect to demonstrate 97% SO_2 removal efficiency and 80% NO_X removal efficiency with scalable modules and to show that our NO_X chemistry is industrially robust. The third phase of the project will take place in the final 21 months wherein

we will concentrate on building and operating a sub-scale proto-type system with a capacity of handling about 100 cubic feet per minute of flue gas. We expect to be able to demonstrate 95% SO_2 removal efficiency with 75% NO_x removal efficiency with the sub-scale prototype.

PROCESS DESCRIPTION

Our concept involves SO_2 scrubbing followed by NO_x scrubbing with regeneration of the individual scrubbing liquors (Figures 1 and 2). The desorbed, concentrated SO_2 and NO_x streams are fed to conventional sulfuric acid and NO_x reduction devices that are not part of the proposed research but which we include for costing estimates as part of the overall process. Both absorption and desorption vessels are based on HFC technology (Figure 3). The basic features of an HFC are that it allows phases to contact without mixing and that there is a large amount of interfacial contact area per unit volume of vessel (Qi and Cussler, 1985). The fiber material (e.g., polypropylene) is hydrophobic, and the fiber walls have small pores (e.g., 0.05 μm) so that gas/liquid contact surface area is created on the liquid side of the pores. Because the walls of the fibers are thin (e.g., 25 μm), there is minimal mass transfer resistance added by the wall of the fiber (diffusion time through the stagnant pore gas is about 0.1 milliseconds). So long as the aqueous phase pressure exceeds that of the gas phase, the interface is stable. The aqueous phase pressure must, however, be kept less than the breakthrough pressure of about 150 psi. Commercially available hollow fibers have sufficiently high mechanical strength to withstand more than 100 psig external pressure and 60 psig internal pressure (Bhave and Sirkar, 197; Majumdar et al., 1988). The fiber wall eliminates entrainment of liquid in the gas and allows independent control of the liquid and gas flow rates. However, the key element of this technology is that the surface area per unit vessel volume is 7 to 30 times higher than that of a traditional packed tower contactor. Consequently, the vessel volume for a given amount of mass transfer is substantially decreased, leading to reduced cost of the scrubber vessel.

Scrubbing SO_2 from flue gases with HFC devices is not new (e.g., Ogundiran et al., 1989; Sengupta et al., 1990). Variants of the HFC technology can, however, be used very efficiently for regenerating these scrubber liquors, and it is this aspect that constitutes part of the novelty of our approach.[1] For regenerating the SO_2 liquor, we intend to contact the liquor with an organic solvent in a hollow fiber contacting device. The organic solvent must have high affinity for SO_2 and very little solubility in water (e.g., dimethyl-aniline). The rationale for using organic extractants is that these have approximately half the heat capacity of water so that the SO_2 can be heat stripped at lower costs (Tung and Kuhr, 1989). These organic liquids cannot be used for direct scrubbing of flue gases because of unacceptably large contamination of the flue gas by the organic solvents.

HFC devices are used so the organic extraction can be done without mixing—so there are no emulsions formed and no phase separation steps required. Further, the high specific contact area results in an extraction vessel much smaller than conventional ones. There are two options for conducting this extraction. In Option A, the SO_2-rich scrubber liquor is passed in the lumen of the HFC, and organic solvent flows on the shell. Sulfur dioxide is preferentially extracted by the organic liquid. The organic liquid is taken to a separate vessel and heated to desorb the SO_2. In Option B, the hollow fibers are divided into two bundles. The SO_2-rich liquor passes down the lumen of one of the bundles, and organic solvent occupies the shell space around the hollow fibers. In the other bundle of hollow fibers, a low pressure is maintained with a small flow of water vapor to draw and sweep the SO_2 through the organic liquid (Figure 4). In this option, no further vessel is required for desorbing the SO_2 from the organic solvent. This particular form of

[1] For the NO_x stripper, however, there is little incentive to use anything other than a conventional stream stripping device. Consequently, we will use conventional technology to regenerate the NO_x liquor.

a hollow fiber contactor is known as a hollow fiber contained liquid membrane, (HFCLM; Majumdar, et al., 1988; Sengupta, et al., 1988).

PROCESS CHEMISTRY

SO_2 Scrubbing. Substantial information exists on the advantages and disadvantages of various chemistries for both SO_x and NO_x absorption (Harkness et al., 1986; Jethani et al., 1990; Oliver and Greenaway, 1989; Roberts and Friedlander, 1980; Oliver, 1989). For wet regenerable SO_2 scrubbing processes, all of the chemistries are essentially different means of providing alkalinity to the solution to induce a high solubility for SO_2 (in the form of HSO_3^- and/or $SO_3^=$. Typical absorbent solutions consist of water with dissolved sodium sulfite (Wellman-Lord process), magnesia, ammonia, sodium sulfide, sodium citrate, soda ash, potassium carbonate, or potassium citrate (Pfizer Sultrol process). We intend to study several of these chemistries and pure water for SO_2 scrubbing.

Whereas these chemistries are well understood, two novel features of the HFC absorber can be exploited to make these chemistries more cost effective than they can be in traditional contactors. First, there are no losses by entrainment of liquor in the flue gas in an HFC device. Second, the liquid/gas flow rate ratio can be much higher in an HFC absorber than in a conventional absorber because the gas and liquid flow rates are independent of each other. Consequently, the concentration of total dissolved alkalinity can be kept lower and still remove the required fraction of SO_2 from the flue gas. Reduced dissolved alkalinity will result in increased lifetime of the SO_2 scrubbing compounds.

NO_x Scrubbing. For NO_x scrubbing, selection of suitable chemistry has been historically one of the most difficult problems. Many unsuccessful attempts have been made to design an ideal scrubbing chemistry. Based on developments in the 1970s, a number of commercial processes have used ferrous chelates based on ethylene-diaminetetraacetic acid (EDTA). Nitric oxide forms a coordination complex with Fe^{2+}-EDTA, and the reaction rates are very fast. Unfortunately, however, as a regenerable process, EDTA chemistry has been proven to be quite expensive because the Fe^{2+} species is oxidized easily to the ineffective Fe^{3+} species. Also a large number of unwanted chemical reactions take place in the scrubber liquor, creating the need for very costly and capital-intensive treatment steps of the scrubbing liquor.

We intend to focus instead on novel water soluble phthalocyanine compounds, developed by SRI, and novel water soluble polymeric derivatives of EDTA, similar to those described by Bedell et al. (1988), both of which we will synthesize in our laboratories. We have already shown under limited flue gas conditions that these compounds bind NO and NO_2 reversibly with no interference from O_2, CO_2, or SO_2.

Finally, one of the potentially greatest advantages of our process (as it relates to process chemistry) is separate SO_2/NO_x scrubbing liquors. This separation will reduce substantially the wide variety of complex side reactions that lead to the need for convoluted regeneration schemes or expensive blowdown in other processes (e.g., Liu et al., 1988).

Extraction of SO_2 from Spent Scrubbing Liquor. The third aspect of the process chemistry is an organic solvent for extracting SO_2 from spent scrubbing liquor. Several suitable solvents are available with a high SO_2 affinity and no propensity to form solid adducts with SO_2: dimethylaniline (DMA), quinoline, and various ethers such as diethylene glycol dimethyl ether (diglyme), triethylene glycol dimethyl ether (triglyme), and tetraethylene glycol dimethyl ether (tetraglyme; Demyanovich and Lynn, 1987). Indeed, DMA and the glymes have been used for commercial absorption processes for SO_2 and H_2S (Kohl and Riesenfeld, 1985). To limit our

effort on this topic, we will restrict ourselves to DMA. To overcome small losses of DMA by volatilization, we will synthesize DMA oligomers.

RESULTS

To date we have worked on six elements of the program: SO_2 scrubbing tests, synthesis of SO_2 and NO_x extraction compounds, their capacity and reversibility tests, spent SO_2 liquor regeneration tests, NO scrubbing tests, and particle deposition tests. Our initial results on some of these elements are presented elsewhere (Gottschlich et. al, 1993). More recent results are discussed next.

SO_2 Scrubbing. Table 1 shows results of SO_2 scrubbing tests. In these experiments, synthetic flue gas containing between 2000 and 2600 ppm SO_2 was fed into the lumens of a 200-fiber, 23-cm long HFC while a 0.2 M aqueous Na_2SO_3 solution was pumped through the shell-side of the HFC. The outlet SO_2 concentration was monitored and showed that the HFC removed between 95-98% SO_2 (See Table 1). Higher removals, upto 99+%, are obtained by optimizing the gas and liquid flowrates.

SO_2 Absorbing Compounds. Table 2 shows several compounds we have synthesized for SO_2 liquor regeneration. The compounds are oligomers of DMA as mentioned above. The SO_2 sorption capacity is expressed as H*, the amount of liquid needed to absorb 1 cm^3 (STP) of SO_2. The smaller this value, the less liquid is needed to treat the flue gas. While imposing the requirements that the liquid be high boiling, with low viscosity, and a small H*, d-DMA is a leading candidate.

SO_2 Spent-Liquor Regeneration. Because of the similar absorption capacity between DMA and d-DMA as shown above, much of our tests for SO_2 liquor regeneration have been with commercially available DMA. Table 3 shows the efficiency of a 1000-fiber HFC in regenerating the spent 0.2 M Na_2SO_3 liquor using DMA. Under optimized conditions, we are able to recover essentially all the SO_2 absorbed in the spent liquor. Note that high flowrates of DMA are required to extract the SO_2.

NO Absorbing Compounds. Table 4 shows equilibrium constants we measured for Fe(II)-EDTA and 5 phthalocyanine compounds. Some of the phalocyanine compounds showed no NO absorption, one showed a higher absorption compared to Fe(II)-EDTA, and another showed lower. The one that showed a higher absorption also showed no oxidation in the presence of 4.5% O_2. Furthermore, it has a solubility 5-10 times higher than Fe(II)-EDTA. The kinetics of the absorption are slower, however, but at elevated temperatures of 50°C, the kinetics are comparable to Fe(II)-EDTA.

NO Scrubbing. Table 5 shows results of NO scrubbing experiments with aqueous solutions of both Fe(II)-EDTA and the phthalocyanine compound above. Under the right conditions, we were able to obtain 85% removal using both compounds. One important result from this set of experiments is that the gas phase offers the most resistance to mass transfer. Additionally, kinetics of the phthalocyanine compound may still play a role, especially at lower temperatures.

Particle Deposition. We have generated 40 mg/ m^3 particles in simulated flue gas by nebulizing a suspension of 0.2 μm (mass average diameter) silica particles. The particle size distribution in the gas stream is shown in Figure 6. In the gas stream, these particles agglomerate to yield a mass average diameter of 0.26 μm. A 10 L/min simulated flue gas containing these particles will be deposited in a 300 fiber HFC. Effect of these particles on the mass transfer will be presented in the paper.

REFERENCES

Bedell, S. A., S. S. Tsai, and R. R. Grinstead, "Polymeric Iron Chelates for Nitric Oxide Removal from Flue Gas Streams," *Ind. Eng. Chem. Res.*, **27**, 2092 (1988).

Bhave, R. R. and K. K. Sirkar, "Gas Permeation and Separation with Aqueous Membranes Immobilized in Microporous Hydrophobic Hollow Fibers," ACS Symposium Series No. 347, in *Liquid Membranes Theory and Applications*, R. D. Noble and J. D. Way, Eds., (American Chemical Society, Washington, DC, 1987) p. 138.

Demyanovich, R. J., and S. Lynn, "Vapor-Liquid Equilibria of Sulfur Dioxide in Polar Organic Solvents," *Ind. Eng. Chem. Res.*, **26**, 548 (1987).

Drummond, C. J., and D. F. Gyorke, "Research Strategy for the Development of Flue Gas Treatment Technology," ACS Symposium Series No. 319, in *Fossil Fuels Utilization: Environmental Concerns*, R. Markuszewski and B. D. Blaustein, Eds., (American Chemical Society, Washington, DC, 1986), p. 146.

Harkness, J.B.L., R. D. Doctor, and R. J. Wingender, "Flue Gas Desulfurization/ Denitrification Using Metal-Chelate Additives," U. S. Patent No. 4,612,175, Sept. 16, 1986.

D. G. Gottschlich, A. S. Bhown, S. Ventura, K. K. Sirkar, S. Majumdar, and D. Bhaumik, "Hollow Fiber Contactors for Simultaneous SO_x/NO_x Removal," Proceedings of the Ninth Annual Coal Preparation, Utilization, & Environmental Control Contactors Conference, Pittsburgh, PA (July 1993).

Jethani, K. R., N. J. Suchak, and J. B. Joshi, "Selection of Reactive Solvent for Pollution Abatement of NO_x," *Gas Separation & Purification*, **4**, 8 (1990).

Kohl, A. and F. Riesenfeld, *Gas Purification*, 4th ed., (Gulf Publishing Company, Houston, 1985).

Liu, D. K., L. P. Frick, and S. G. Chang, "A Ferrous Cysteine Based Recyclable Process for the Combined Removal of NO_x and SO_2 from Flue Gas," *Env. Sci. and Technol.*, **22**, 219 (1988).

Majumdar, S., A. K. Guha, and K. K. Sirkar, "A New Liquid Membrane Technique for Gas Separation," *AIChE J.*, **34**, 1135 (1988).

Ogundiran, O. S., S. E. Le Blanc, and S. Varanasi, "Membrane Contactors for SO_2 Removal from Flue Gases," Pittsburgh Coal Conference, September 1989.

Oliver, E. D., "NO_x Removal," SRI International Process Economics Program Report No. 200 (May 1989).

Oliver, E. D. and D. Greenaway, "SO_2 Removal from Flue Gas," SRI International Process Economics Program Report No. 63C (December 1989).

Qi, Z. and E. L. Cussler, "Microporous Hollow Fibers for Gas Absorption," *J. Membr. Sci.*, **23**, 321 (1985).

Roberts, D. L. and S. K. Friedlander, "Sulfur Dioxide Transport Through Aqueous Solutions," *AIChE J.*, **26**, 593-610 (1980).

Sengupta, A., R. Basu, and K. K. Sirkar, "Separation of Solutes from Aqueous Solution by Contained Liquid Membranes," *AIChE J.*, **34**, 1698 (1988).

Sengupta, A., B. Raghuraman, and K. K. Sirkar, "Liquid Membranes for Flue Gas Desulfurization," *J. Membr. Sci.*, **51**, 105 (1990).

Tung, S. E. and R. W. Kuhr, "Flue Gas Desulfurization Test Facility," presented at the Fifth Annual Coal Preparation, Utilization, and Environmental Control Contractors' Conference, Pittsburgh, PA, July 31-August 3, 1989.

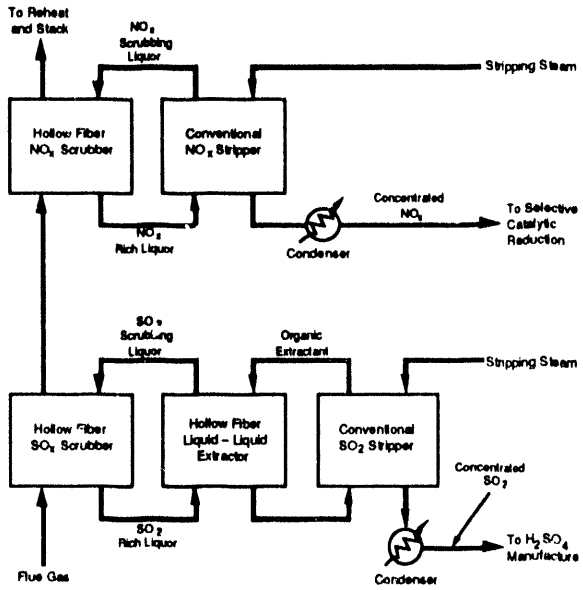

Figure 1. Proposed SO_x /NO_x wet scrubbing with hollow fiber contacting devices. (Option A for SO_2 liquor regeneration)

SO_2 liquor regeneration occurs in hollow fiber liquid – liquid extraction (LLE) device.

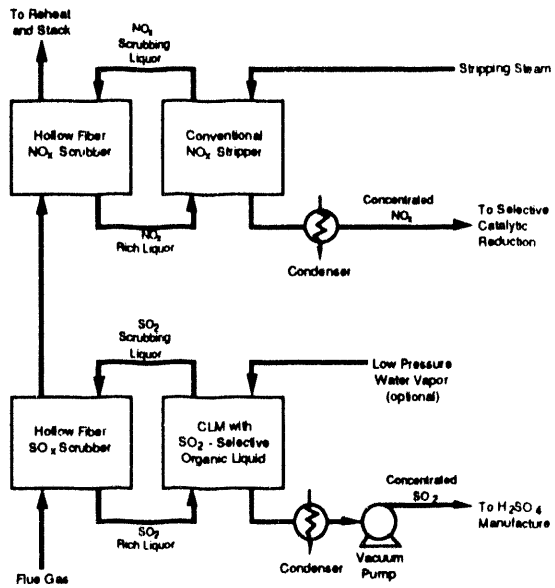

Figure 2. Proposed SO_x /NO_x wet scrubbing with hollow fiber contacting devices. (Option B for SO_2 liquor regeneration)

SO_2 liquor regeneration occurs in hollow fiber contained liquid membrane (CLM) device. Condenser/vacuum pump system combine to give driving force for operation of CLM.

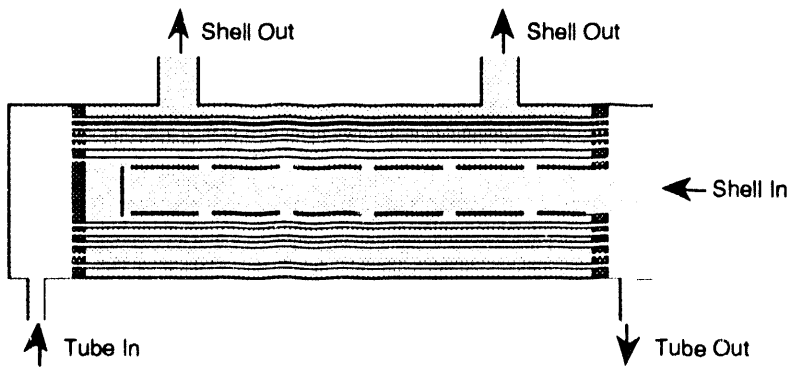

Figure 3. Schematic diagram of the crossflow hollow fiber contactor (HFC) module.

Liquid flows through the shell-side and gas through to tube-side.

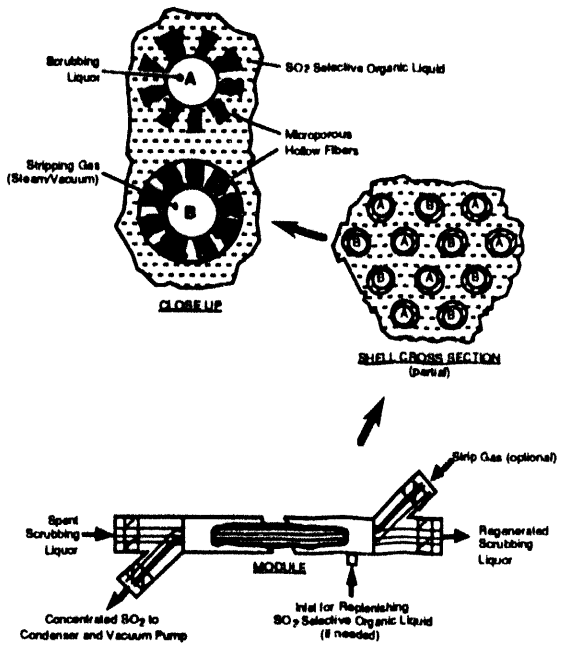

Figure 4. Hollow fiber contained liquid membrane for regenerating SO_2 scrubber liquor.

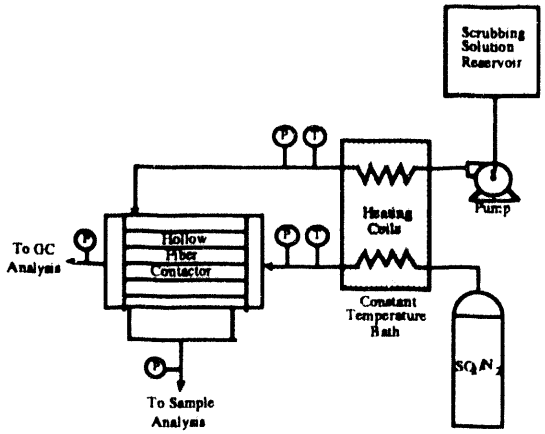

Figure 5. Schematic diagram of HFC test apparatus.

Figure 6. Particle Size Distribution of Dispersed Silica in Simulated Flue Gas

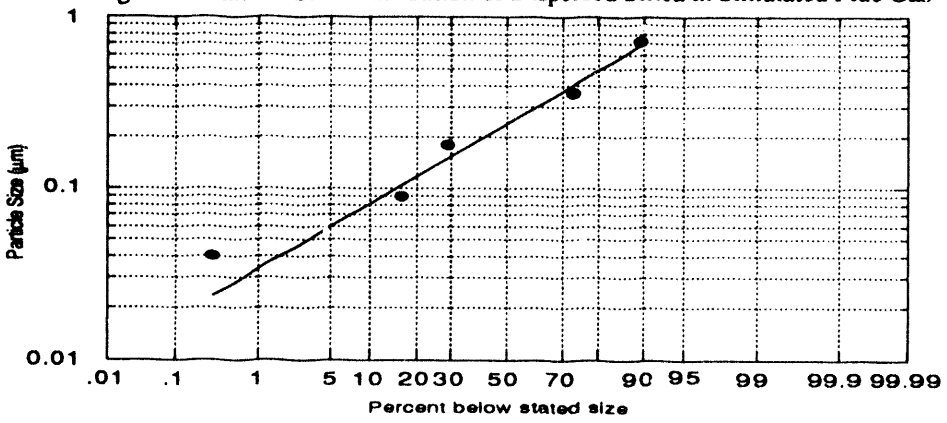

Table 1. SO_2 ABSORPTION BY 0.2 M Na_2SO_3 IN A 200-FIBER MODULE

Run No.	Liquid Flow-rate, mL/min	Gas Flow-rate, sccm	SO_2 Composition, ppm		% Removed
			Inlet	Outlet	
1	5.3	1809	2430	115	95
6	5.1	1809	2610	55	98
12	20	2713	2050	65	97
AE-4	20	2272	2250	69	97
AE-6	10	2372	2300	100	96

Table 2. RESULTS FOR SO_2-ABSORBING COMPOUNDS

Compound	Temperature, °C	H*, cm^3liq/ cm^3SO_2(STP)	Comments
DMA	35	0.36-0.43	BP = 194°C
d-DMA	35	0.36-0.44	BP>>300°C
MAPA	80	Complete sorption	Irreversible
AMAPA	80	0.21-0.31	Viscous
d-siloxane	35	0.36-0.60	Expensive
p-siloxane	35	0.28-0.46	Expensive

Table 3. RESULTS FOR SO_2-ABSORBING COMPOUNDS

Run No.	0.2 M Na_2SO_3 Flowrate, mL/min	DMA Flowrate, mL/min	% SO_2 Recovered
AE-10	10	38	52.6
AE-11	50	42	92.9
AE-12	20	102	~100

Table 4. EQUILIBRIUM CONSTANTS FOR NO_X-ABSORBING COMPOUNDS
R + NO = R·NO

Compound	Temperature, °C	K, L/mol	Comments
Fe(II)-EDTA	35	9.86×10^5	Oxidizes to Fe(III) in presence of O_2
1-Ph	25	0	No absorption
2-Ph	25	3.41×10^5	
3-Ph	25	2.03×10^6	No oxidation in presence of O_2
4-Ph	25	0	No absorption
5-Ph	25	0	No absorption

Table 5. NO_X SCRUBBING WITH 300-FIBER HFC

Feed Gas			Scrubbing Liquid 20 mM, 25°C		
NO (ppm)	O_2 (%)	Flowrate (sccm)	Type	Flowrate (mL/min)	% Removal
500	4.5	900	3-Ph	6.7	22
500	4.5	100	3-Ph	4.6	51
2300	4.5	100	3-Ph	4.1	62
500	4.5	40	3-Ph	4.1	50
500	4.5	40	3-Ph	0.5	50
500	4.5	100	3-Ph (100 mM 50°C)	1.1	85
100	0	290	Fe(II) EDTA	146	80
100	0	200	Fe(II) EDTA	25	85